Malformations of Cortical Development

4

Human cerebral cortical development is a complex process and occurs in three overlapping stages, namely, neuronal proliferation, migration and organisation.

Neuronal proliferation (6–16 weeks gestational age) is the differentiation of stem cells in the periventricular subependymal layer (germinal matrix) into neuroblasts.

The neuroblasts migrate outwards along the radial glial scaffolding to reach and populate the future cortex from the innermost layer outwards. This process, termed neuronal migration, results in the formation of the normal six-layered (hexalaminar) cortex. Neuronal migration begins at 6 weeks of gestation and continues postnatally till 5 months of age. Sulcation and gyration are directly related to neuronal migration and serves to maximise the cortical surface area without increasing the brain volume.

The phase of neuronal organisation (20 weeks gestational age to postnatal life) involves separation of neurons from the radial glial fibres, dendrite and axonal formation and establishment of synaptic connections.

The above processes are regulated by specific genes and complex signalling pathways. Malformation of cortical development may be caused by a genetic abnormality, infection, teratogen or trauma. Knowledge of the genetic basis is essential for prenatal molecular confirmation by invasive testing.

Malformations of cortical development (MCD) may be broadly classified as:

Phase of development	Disorders
Neuronal proliferation	Microcephaly Megalencephaly
Neuronal migration	Heterotopia Lissencephaly Cobblestone malformation Hemimegalencephaly
Neuronal organisation	Polymicrogyria Schizencephaly

A particular MCD may be a combination of any of the disorders mentioned above. An excellent example is the association of periventricular heterotopia with polymicrogyria. The genes that control cortical development may also be involved in the development of other organ systems of the body. Hence associated anomalies in the eyes, hindbrain, face and skeletal system, if detected, may help to make a specific diagnosis. For example, classical lissencephaly with dysmorphic facies, congenital heart disease and polydactyly is indicative of Miller-Dieker syndrome. Mild lateral ventriculomegaly is very often the first finding seen in the US examination done at 18–20 weeks. Sulcation is just about beginning at this stage. Repeat scan at 26 weeks is necessary to recognise sulcatory landmarks as well as to reassess the lateral ventricular size.

4.1 Disorders of Neuronal Proliferation

4.1.1 Microcephaly

Impairment of neuronal proliferation (decrease in the number of progenitor cells in the germinal matrix) results in a small-sized brain which is reflected as a small-sized head. The causes are varied and include single gene/syndromic disorders (autosomal dominant/recessive, X-linked recessive forms), chromosomal abnormalities and infections (CMV and toxoplasma). Hydantoin and aminopterin teratogenicity, maternal phenylketonuria and maternal alcohol abuse can cause microcephaly in the fetus.

The ultrasound findings are as follows:

1. Head circumference (HC) of −3SD or lesser at any gestational age is indicative of microcephaly. Progressive growth lag of HC seen on serial monitoring at three to four weekly intervals is confirmatory in cases with borderline HC (Figs. 4.1a, b, 4.2 and 4.3).
2. Primary microcephaly is diagnosed when there are no associated intracranial or extracranial abnormalities.
3. Microcephaly may manifest early or late in pregnancy. In a significant number of cases, the HC may become lesser than the cut-off of −3SD in the third trimester or during the first few years of life (Fig. 4.2).

B. S. Rama Murthy, *Imaging of Fetal Brain and Spine*, https://doi.org/10.1007/978-981-13-5844-9_4

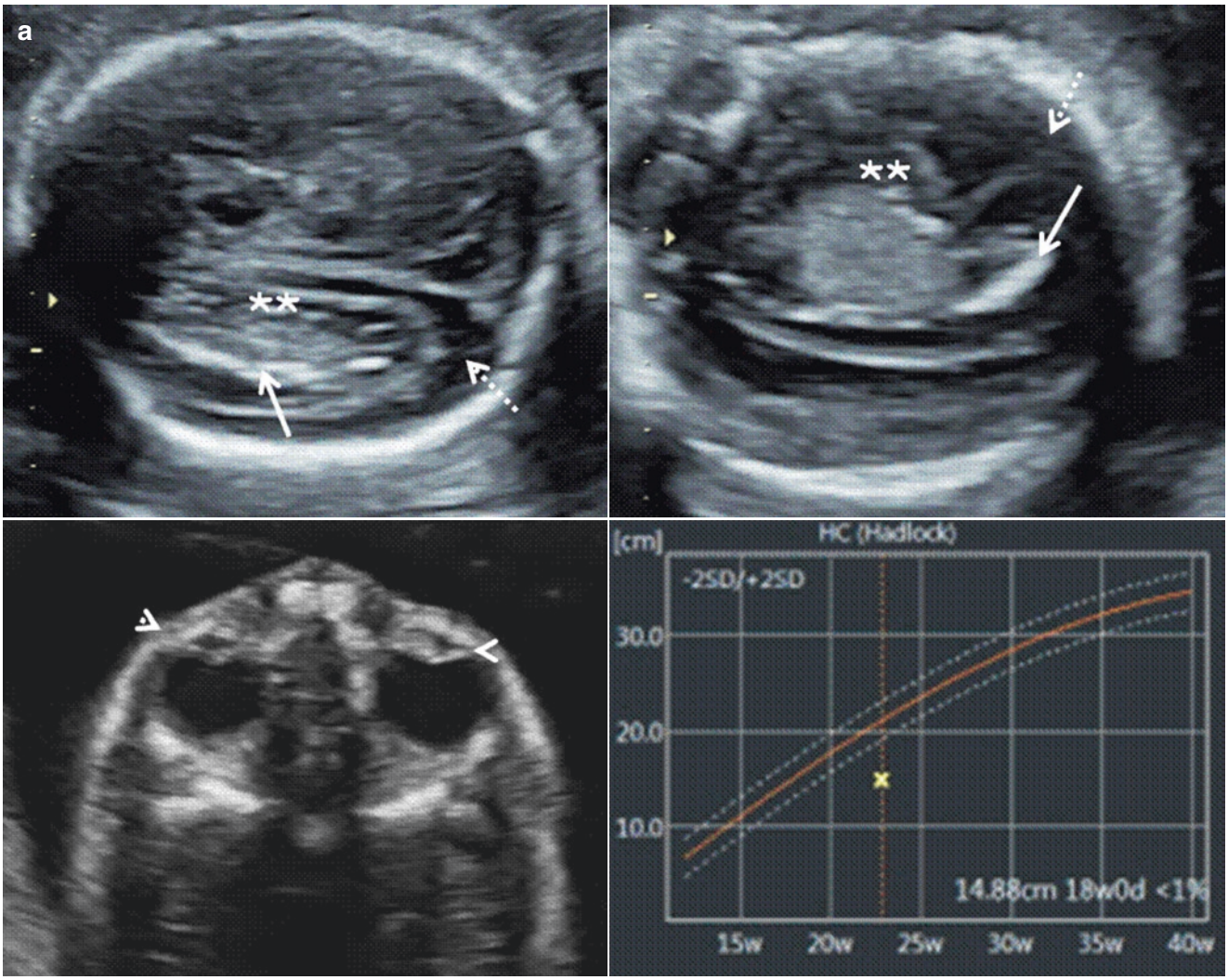

Fig. 4.1 (**a**) 23 weeks (TAS) *microcephaly* – axial transventricular and oblique sections of cranium, axial section of orbits and head circumference growth curve – thin cerebral parenchyma with no sulcation (**), increased subarachnoid space (dotted arrows), bilateral periventricular calcification (solid arrows), bilateral cataract (arrowheads), HC less than −3SD. Maternal serology is positive for CMV. (**b**) 23 weeks (TAS) *microcephaly* – midsagittal section of face (profile), 3D surface rendering of the head and face, lateral and oblique rotational views, right upper limb and both lower limbs – receding forehead is seen in facial 2D and 3D views, right clenched fist (arrowhead), flexion contracture of right elbow (solid arrow) (right fist not seen due to flexion contracture of the wrist) and adduction contractures of both hips (dotted arrows)

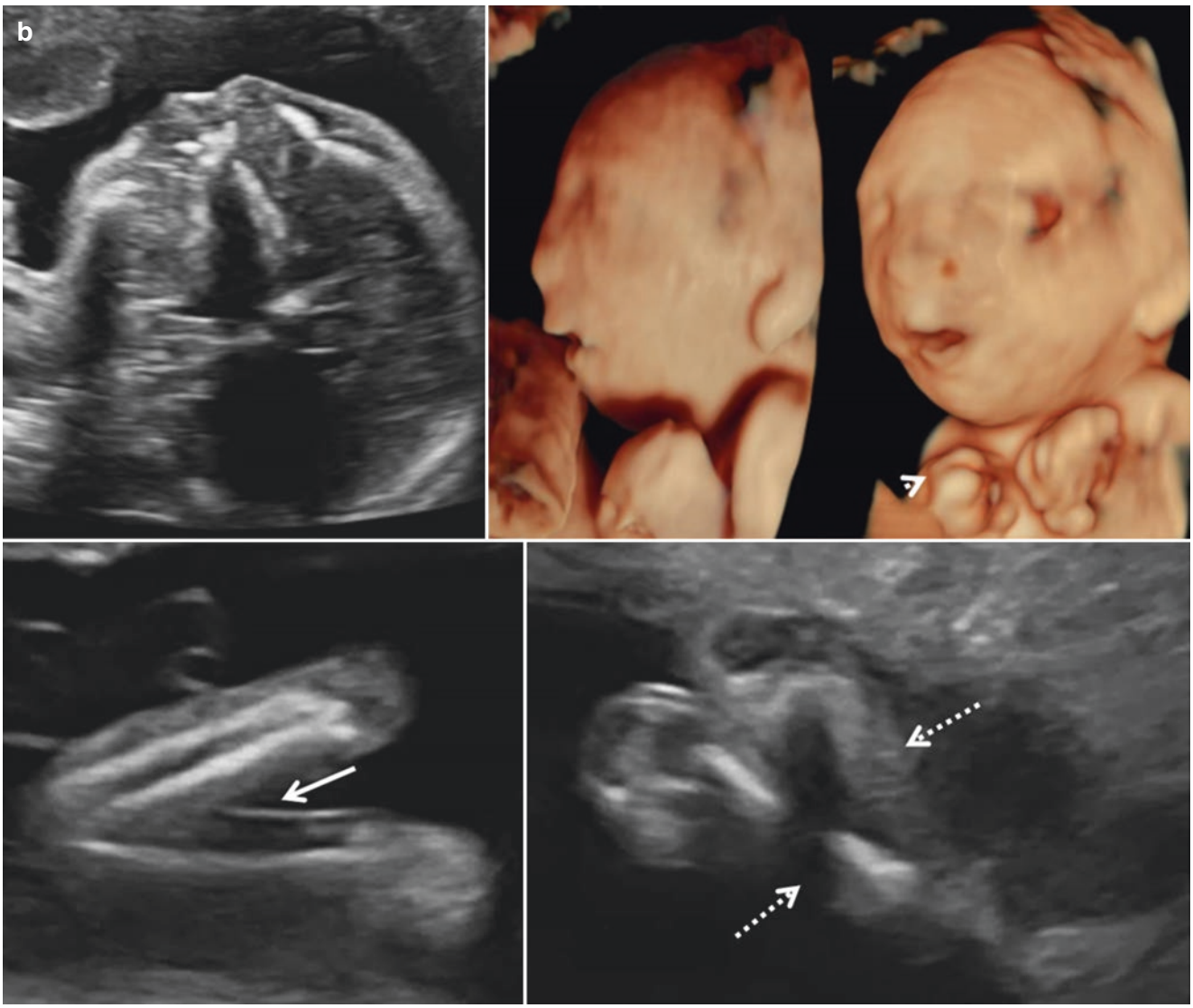

Fig. 4.1 (continued)

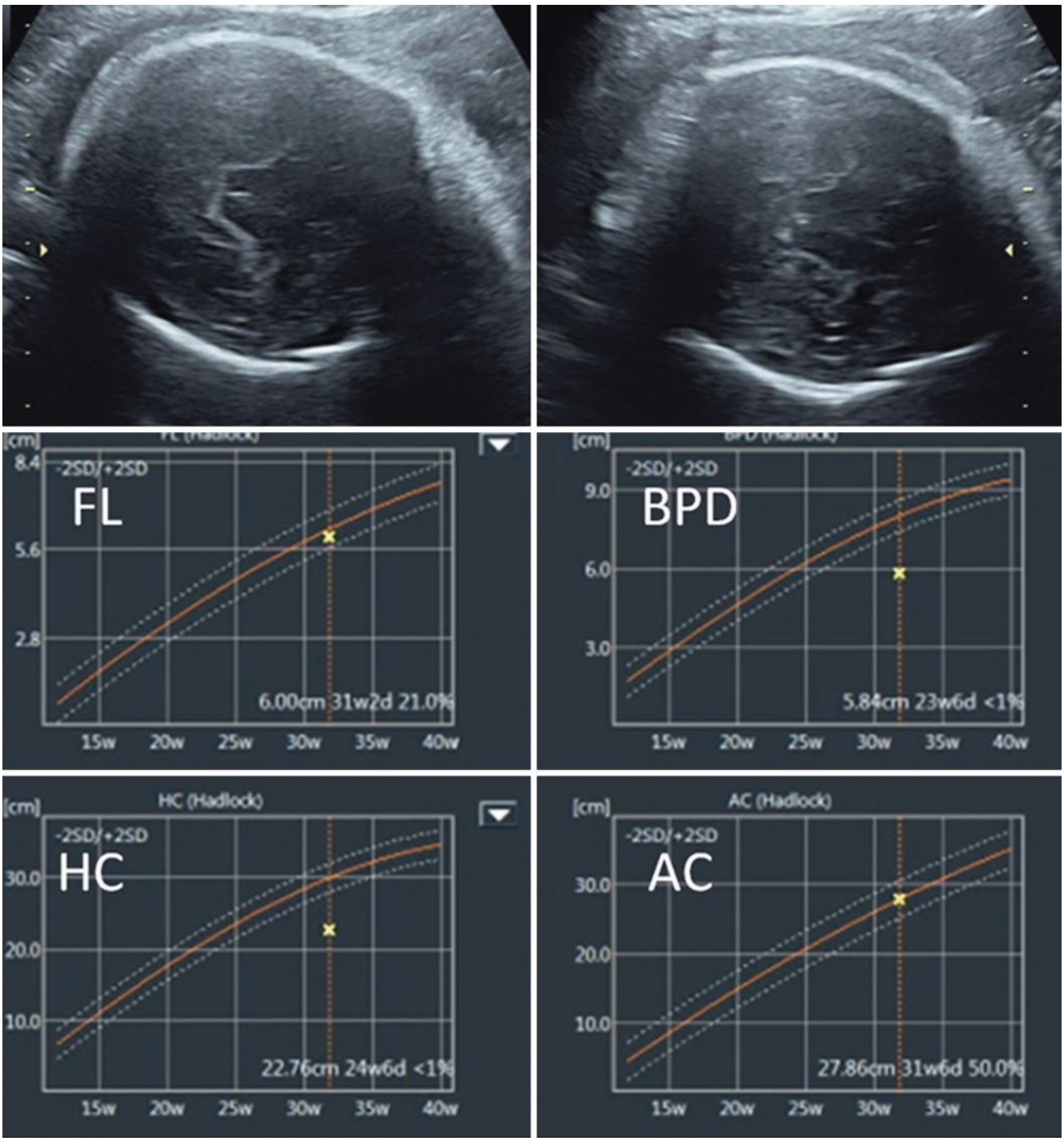

Fig. 4.2 31 weeks (TAS) *microcephaly* – axial transventricular sections – inability to visualise the intracranial structures, growth curves demonstrate HC less than –3SD

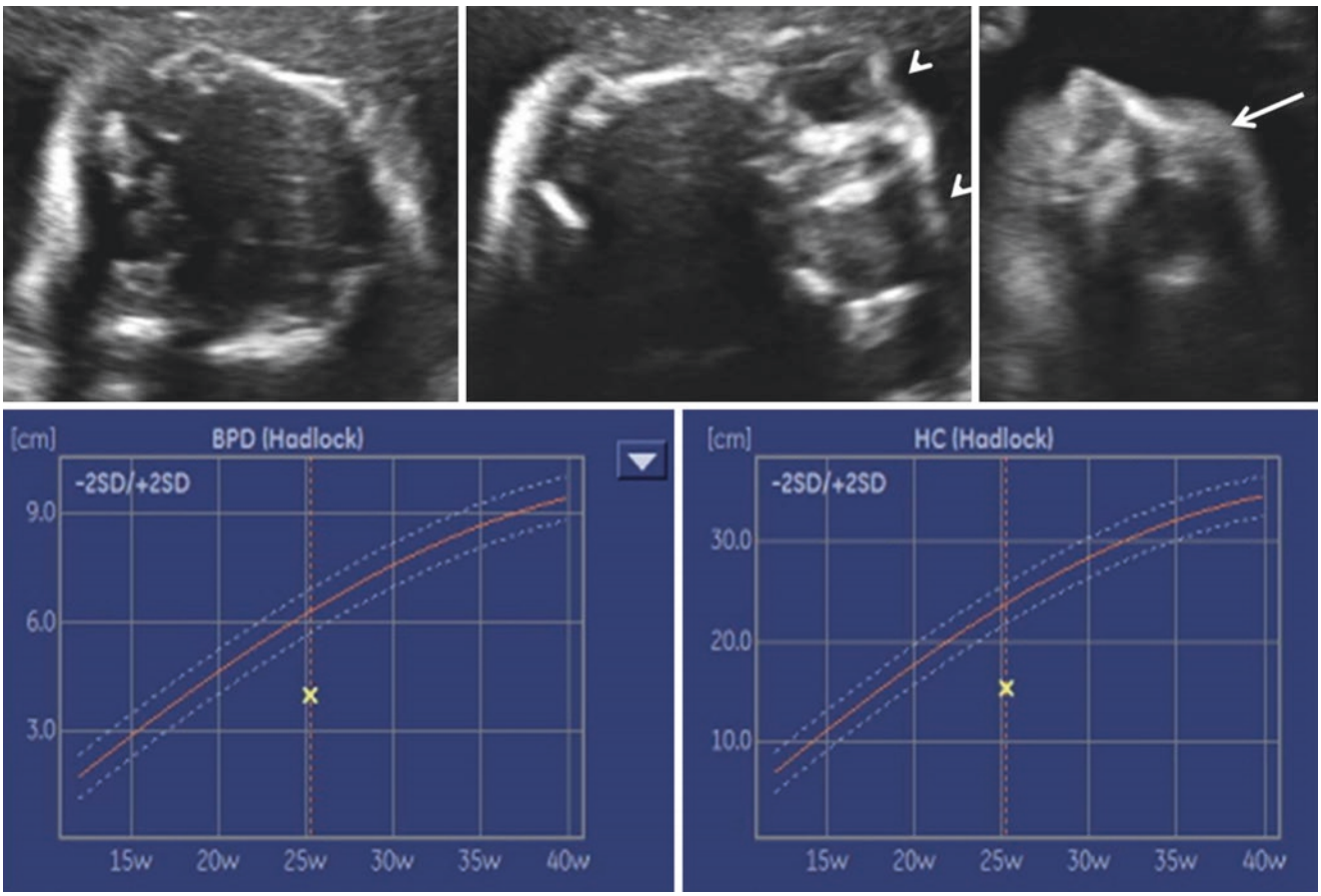

Fig. 4.3 25 weeks (TAS) *severe microcephaly* – transverse section of cranium, axial orbital section, midsagittal facial profile section – inability to visualise intracranial structures, relatively large orbits (arrowheads), severely receding forehead (solid arrow), extreme lag of biparietal diameter and head circumference

4. Receding forehead (due to frontal lobe hypoplasia) is seen in the midsagittal section of the face (Fig. 4.1a, b).
5. The intracranium may be difficult to visualise due to poor acoustic window as the calvarial sutures are narrow (Fig. 4.3).
6. Increased subarachnoid space, lissencephaly, holoprosencephaly, periventricular heterotopia, polymicrogyria, hydrocephaly, callosal abnormalities and infection sequelae (Fig. 4.1a, b) may be seen.

Counselling by a geneticist with fetal karyotyping/chromosomal microarray, infection screening and possible molecular testing should be considered.

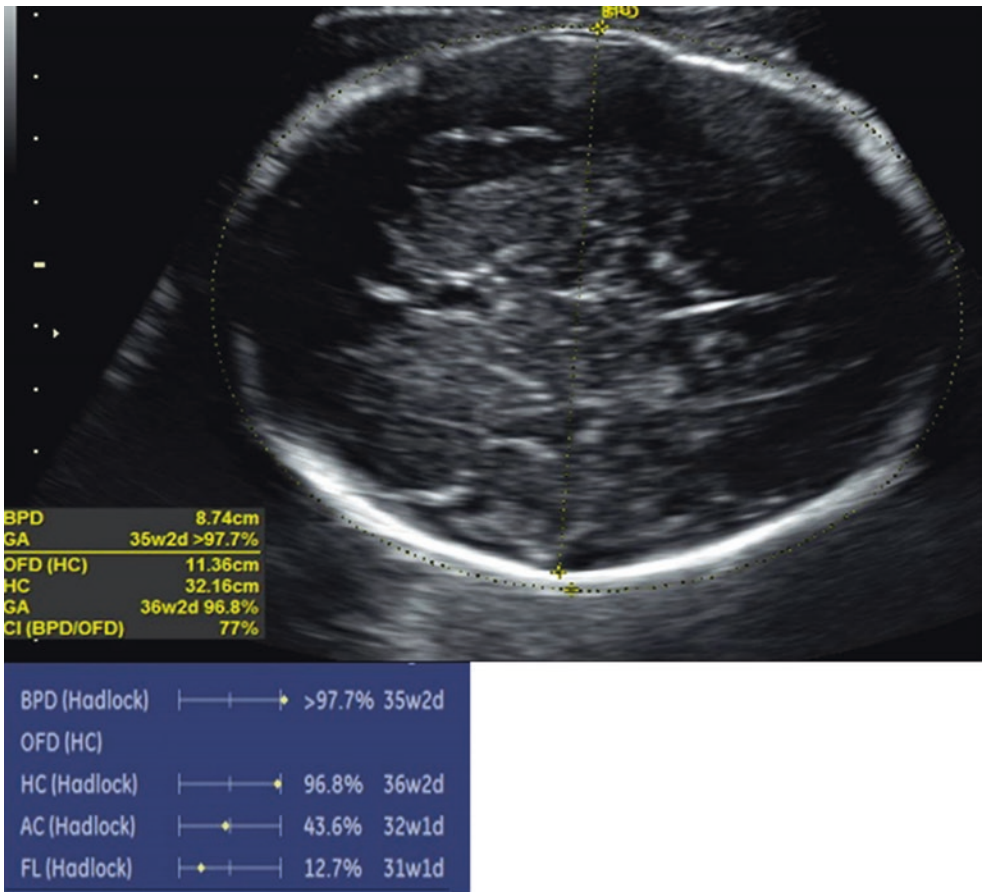

Fig. 4.4 33 weeks (TAS) *macrocephaly* – axial transthalamic section – more than 98th percentile head circumference with normal intracranial findings

4.1.2 Macrocephaly

Rapid cell proliferation or decreased cell apoptosis results in an increase in the number of the neurons produced. This results in a large brain and large cranium.

The ultrasound findings are as follows:

1. HC is more than 98th percentile (Fig. 4.4).
2. Hydrocephalus, intracranial tumors, subdural bleed and malformations of cortical development should be excluded.
3. Most cases present in the third trimester with HC being normal in the second trimester.
4. Increased subarachnoid space is a feature of benign familial macrocephaly. Family history of a large head should be sought for as benign familial macrocephaly is inherited as an autosomal dominant or recessive trait.
5. Rarely macrocephaly could be part of a syndrome such as Sotos syndrome or skeletal dysplasia like achondroplasia and thanatophoric dysplasia.
6. As diagnosis is usually made in the third trimester, a thorough examination of the intracranium is often not possible by ultrasonography. In these instances, fetal MRI may help to assess the intracranium better.
7. Serial monitoring of HC at four weekly intervals should be planned in cases where there is a suspicion (borderline HC).
8. Majority of fetuses with macrocephaly with normal intracranial findings do well postnatally.

4.2 Disorders of Neuronal Migration

Disorders of neuronal migration are mostly due to genetic etiology. The causative gene mutation results in defective initiation or migration or arrest which manifests as periventricular heterotopia or classical lissencephaly or cobblestone malformation, respectively (Fig. 4.5).

Lissencephaly is a lack of or poor sulcation and gyration resulting in a smooth brain. The genetic abnormality that causes lissencephaly may also result in abnormalities in the corpus callosum and cerebellum. Detailed neurosonography is indicated when a neuronal migration disorder is suspected. Suspicion may be aroused by any of the following:

1. Family history
2. Finding or findings on basic US examination:
   (a) Mild lateral ventriculomegaly
   (b) CSP abnormalities

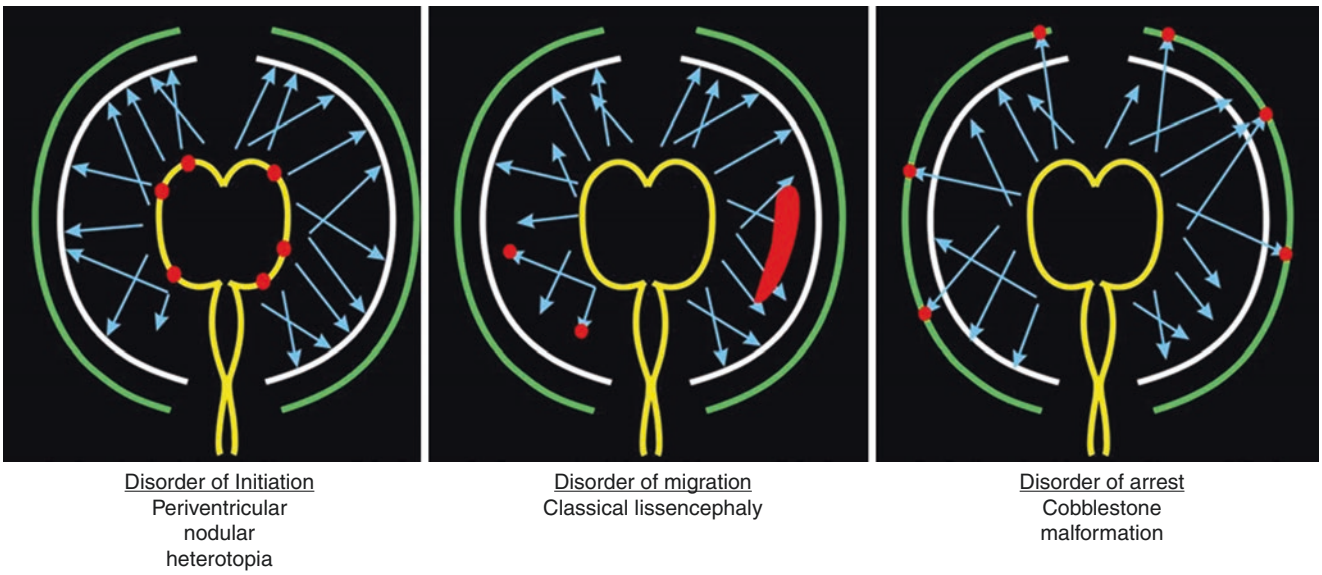

Fig. 4.5 Schematic diagram of the pathogenesis of malformation of neuronal migration. Periventricular zone (yellow line), nodular heterotopia (red dots), band heterotopia (red band), pia mater (green line)

(c) Irregular ventricular wall
(d) Thin cerebral mantle
(e) Microcephaly or macrocephaly

Fetal MRI may supplement the findings seen on detailed neurosonogram.

4.2.1 Classical Lissencephaly

In classical lissencephaly (type I lissencephaly), the radial migration is defective, and neurons fail to reach the cortical surface. This results in poor or absent sulcation and gyration. LIS1 gene mutation (autosomal dominant) is the commonest mutation causing classical lissencephaly. Deletion of genes in the region (17p13.3) contiguous with the LIS1 gene mutation results in Miller-Dieker syndrome which is classical lissencephaly with facial dysmorphism. LIS1 gene mutations are of de novo origin in most cases. DCX gene mutation (X-linked dominant) results in full-blown classical lissencephaly in the male and milder disease in the female (subcortical band heterotopia or double cortex). ARX mutation (X-linked dominant) results in classical lissencephaly with genital ambiguity. RELN mutation (autosomal recessive) causes classical lissencephaly with cerebellar hypoplasia. A working knowledge of these genetic abnormalities helps to look for associated anomalies and recognising patterns. Molecular testing can be tailored on a case-to-case basis.

The anatomic abnormalities can only be detected at or after a gestational age when a particular sulcatory landmark should be seen. For example, acute angle shape of the lateral fissure and appearance of cerebral convexity sulci are seen normally by 26 weeks. Hence, delay or failure of these sulcatory events can only be recognised at 26 weeks or later.

The ultrasound findings are as follows:

1. Figure of eight or hourglass configuration of the brain on axial sections due to its small size (micrencephaly) and absent operculation of the lateral fissure (Fig. 4.12a, b).
2. Delayed (shallow for gestational age) or absent sulcation is detected by a systematic study of the medial hemispheric sulci (parieto-occipital, calcarine and cingulate), lateral fissure and convexity sulci (central, pre- and postcentral and temporal) (Figs. 4.6a–d, 4.7a, b and 4.8a, b). Widely spaced shallow sulci and broad gyri are termed pachygyria.
3. Mild lateral ventriculomegaly and abnormal shape of the lateral ventricle may be seen particularly on coronal sections (Figs. 4.6a–d and 4.7a, b).
4. Complete or partial callosal agenesis and callosal hypoplasia may be present and can be detected on the midsagittal section (Figs. 4.9a, b and 4.10a, b).
5. Associated cerebellar hypoplasia (Fig. 4.11a, b) and ambiguous genitalia help in suspecting RELN and ARX gene mutations, respectively.
6. X-linked genetic basis should be considered if the condition is recurrent and the fetal sex is male.
7. In Miller-Dieker syndrome, in addition to the classical lissencephaly, there could be facial dysmorphism (frontal bossing, hypertelorism, small upturned nose, protuberant arched upper lip, small jaw), IUGR, polyhydramnios, congenital heart defects, polydactyly and cryptorchidism (Fig. 4.12a, b). FISH testing for the 17p13.3 microdeletion on the amniotic fluid is diagnostic of the condition.

8. Tubulin genes encode tubulin proteins which are fundamental components of microtubules. Microtubules participate in intracellular transport, cell division, and neuronal migration. The tubulin genes include TUBA1A, TUBA8, TUB2B, TUBB3, TUBBS and TUBG1. Mutations in the tubulin genes result in a spectrum of abnormalities termed 'tubulinopathies'. These disorders manifest as combinations of cortical defect (lissencephaly, microlissencephaly or polymicrogyria), subcortical defect (CACC, PACC or callosal dysgenesis) and cerebellar or brain stem hypoplasia.

Fetal MRI can confirm US findings.

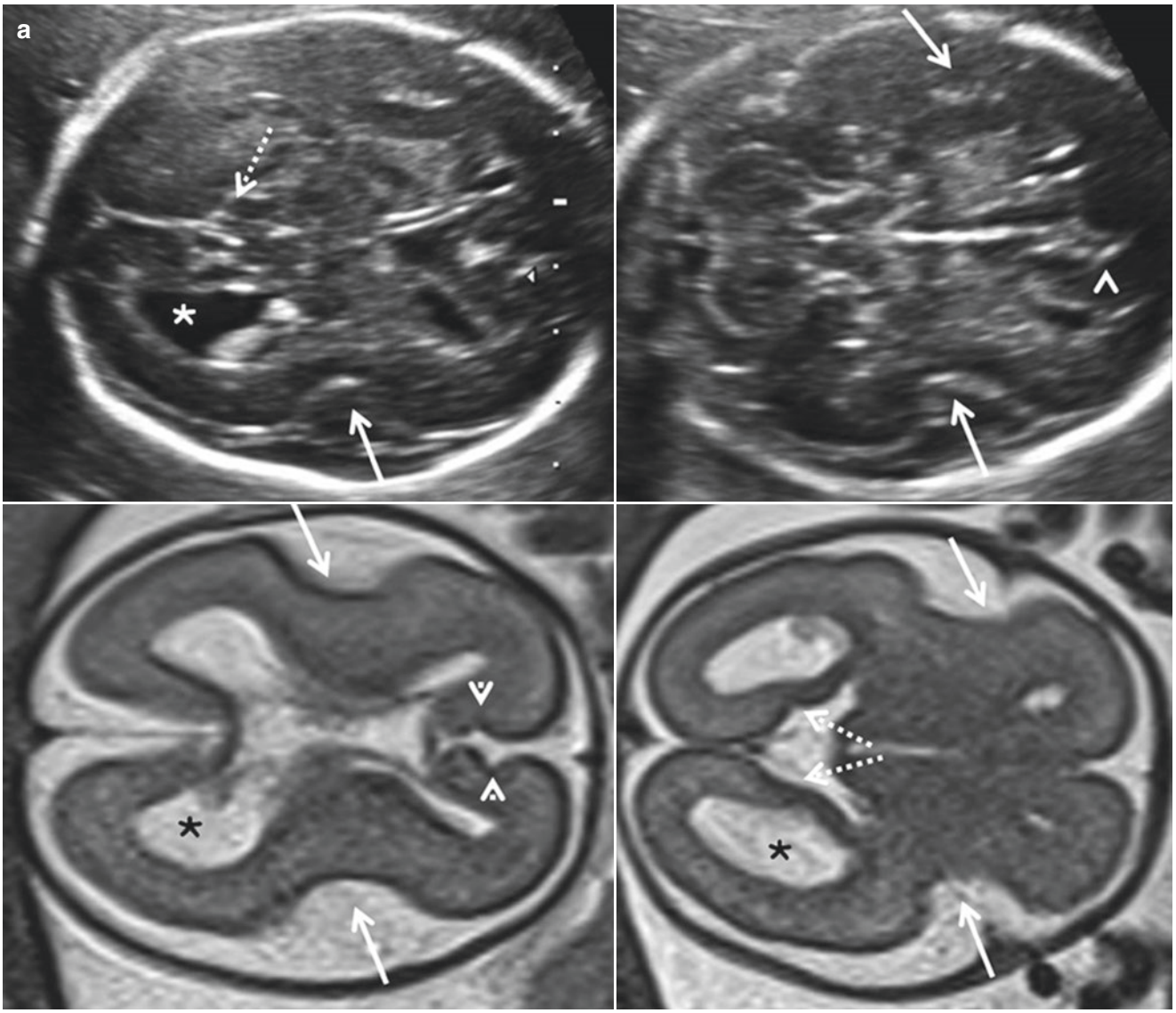

Fig. 4.6 (**a**) 26 weeks (TAS and MRI) *classical lissencephaly* – axial transventricular and transcerebellar US and T2W sections – mild left lateral ventriculomegaly (*), atrial diameter of 11 mm, obtuse-angled lateral fissure (solid arrows), parieto-occipital sulcus (dotted arrows) and cingulate sulcus (arrowheads) are wider than taller indicating lag in development. (**b**) 26 weeks (TAS and MRI) *classical lissencephaly* – coronal transfrontal, transcaudate and transthalamic US and T2W sections – obtuse-angled shape of lateral fissure (solid arrows), abnormal shape of lateral ventricles (dotted arrows). (**c**) 26 weeks (TAS and MRI) *classical lissencephaly* – left and right parasagittal US and T2W sections – mild left lateral ventriculomegaly (*), convexity sulci absent (solid arrows), abnormal shape of left posterior horn (dotted arrows). (**d**) 26 weeks (TAS and MRI) *classical lissencephaly* – midsagittal US and T2W sections – corpus callosum is normal (solid arrows)

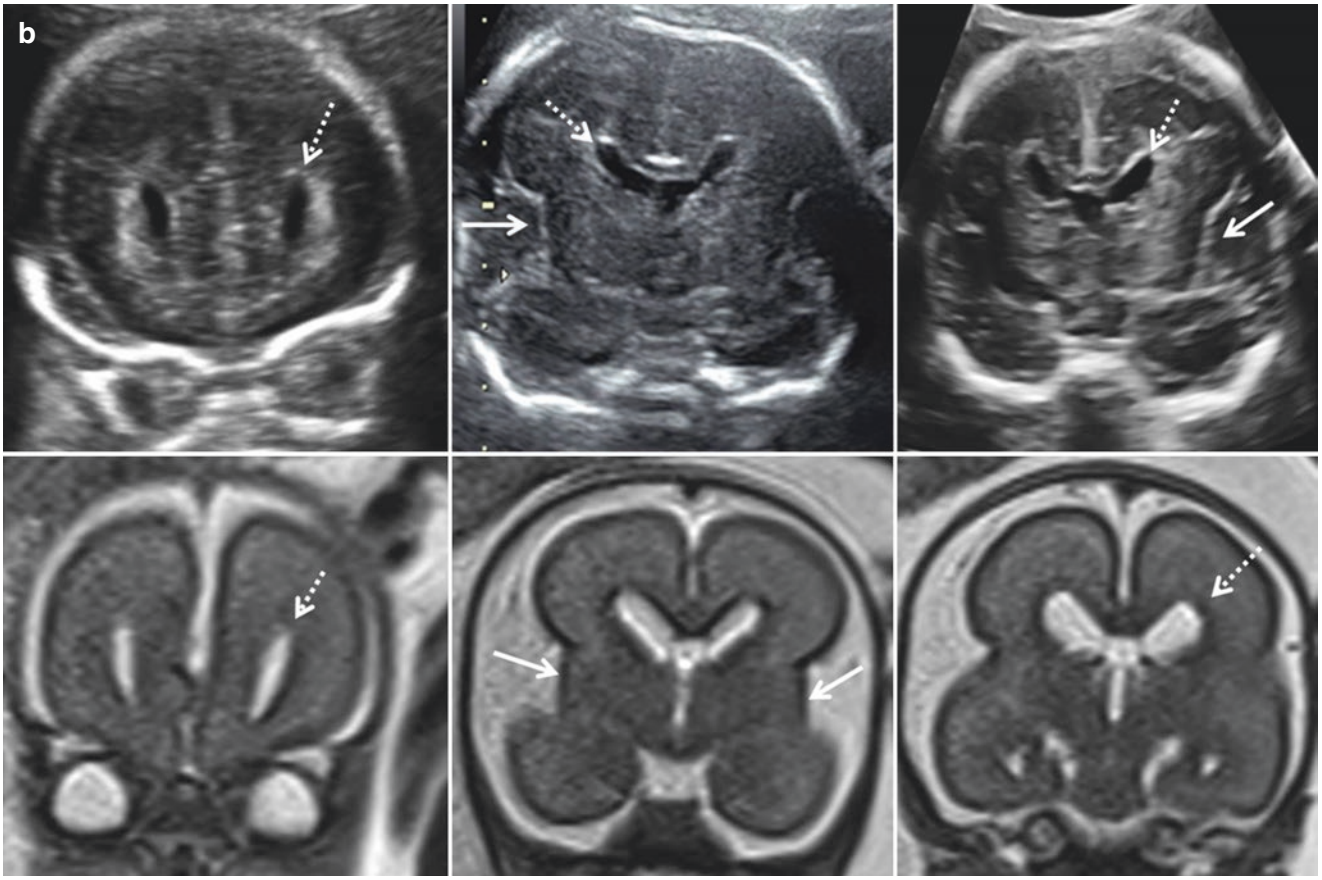

Fig. 4.6 (continued)

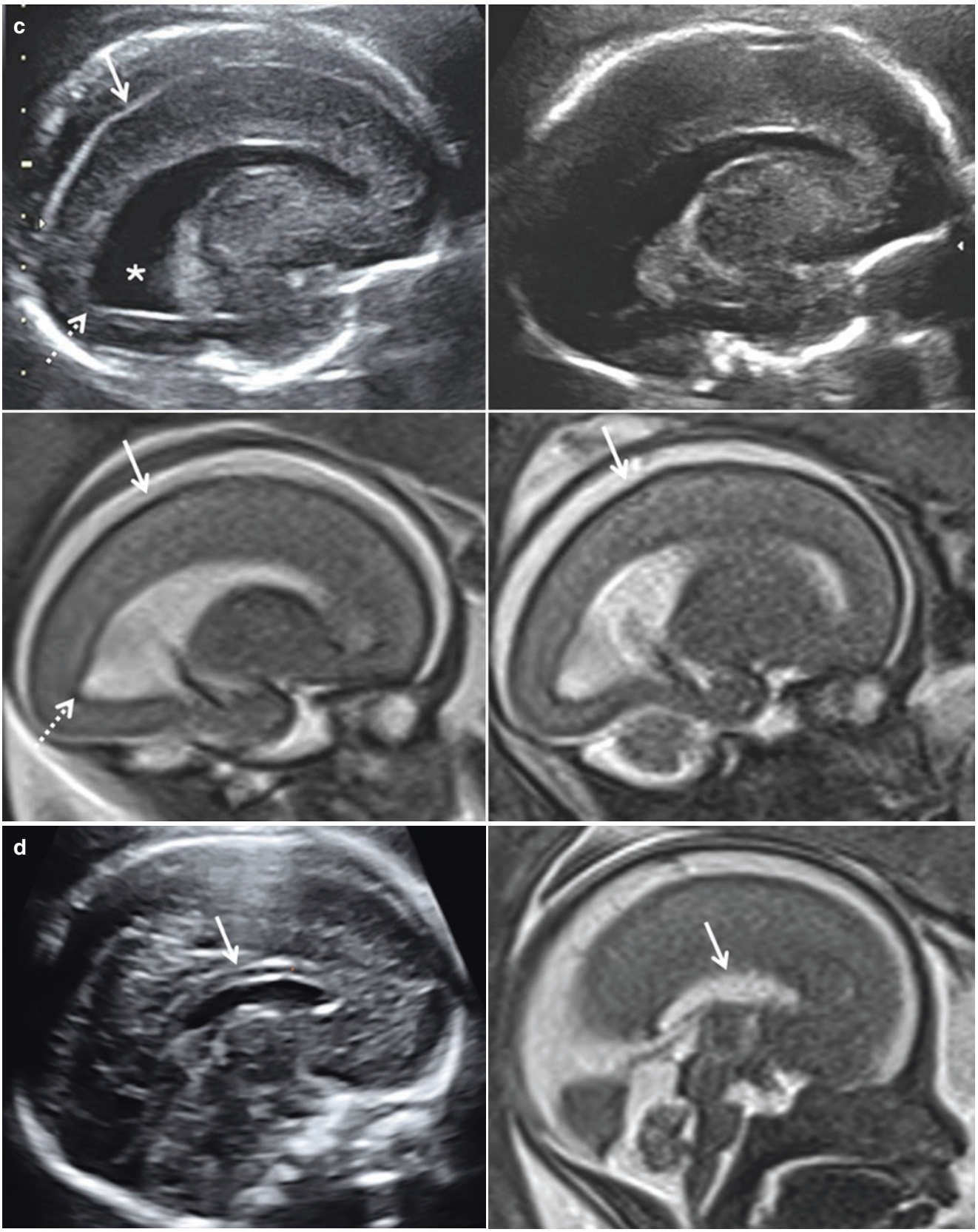

Fig. 4.6 (continued)

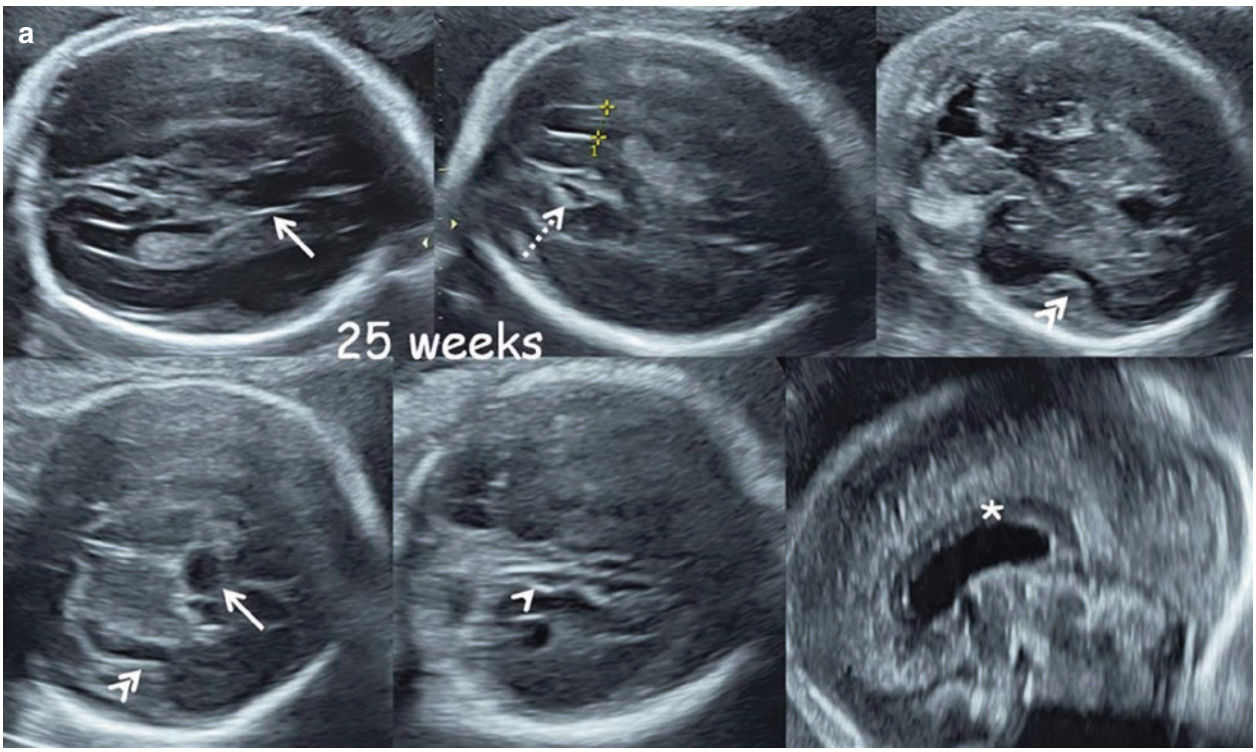

Fig. 4.7 (**a**) 25 and 27 weeks (TAS) *classical lissencephaly* – axial transventricular and transcerebellar sections, coronal transcaudate and transcerebellar sections and midsagittal section – lateral ventricles are normal, CSP is wide (solid arrows), parieto-occipital (dotted arrow) and calcarine (arrowhead) sulci are shallow indentations, lateral fissure is shallow and obtuse angled in shape (double arrowheads), corpus callosum is normal (*). (**b**) 25 and 27 weeks (TAS and MRI) *classical lissencephaly* – axial transventricular and transcerebellar sections, coronal transcaudate and transcerebellar sections and parasagittal section – lateral ventricles are normal, CSP appears wide (*), no progress in the development of parieto-occipital sulci (dotted arrows) and calcarine sulci (single arrowhead), lateral fissure continues to be shallow and obtuse angled (double arrowheads), convexity sulci have not appeared (solid arrow). No progress in sulcation when compared to the 25 weeks study. (**c**) 25 and 27 weeks (TAS and MRI) *classical lissencephaly* – axial transventricular, coronal transcaudate and parasagittal T2W sections – lateral ventricles are normal, CSP appears wide (*), parieto-occipital sulci (dotted arrow) are barely visualised, lateral fissure is shallow and obtuse angled (double arrowheads), cerebral convexity sulci have not appeared (solid arrow). US findings are confirmed by MRI. Note that the MRI was planned at 27 weeks rather than 25 weeks

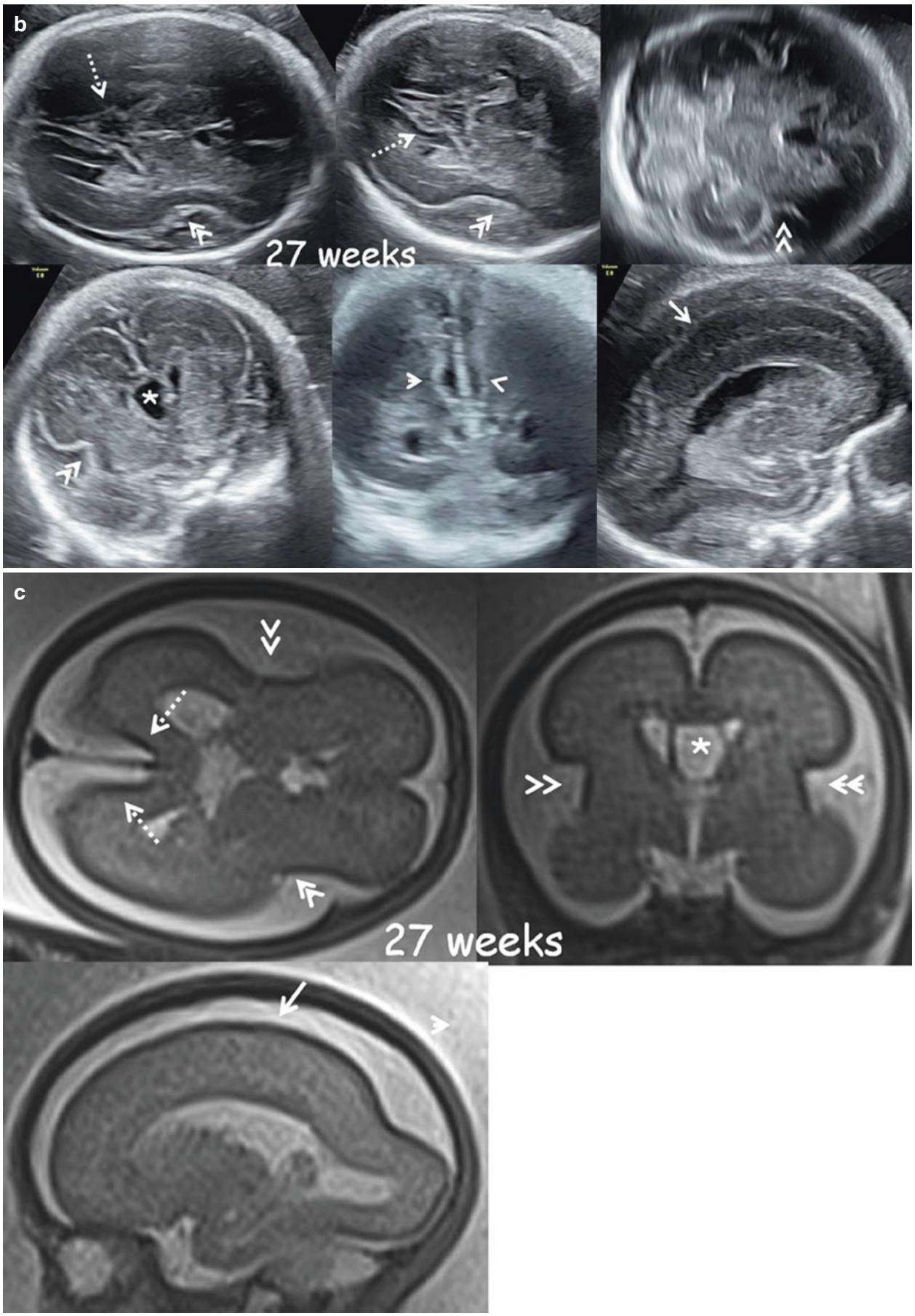

Fig. 4.7 (continued)

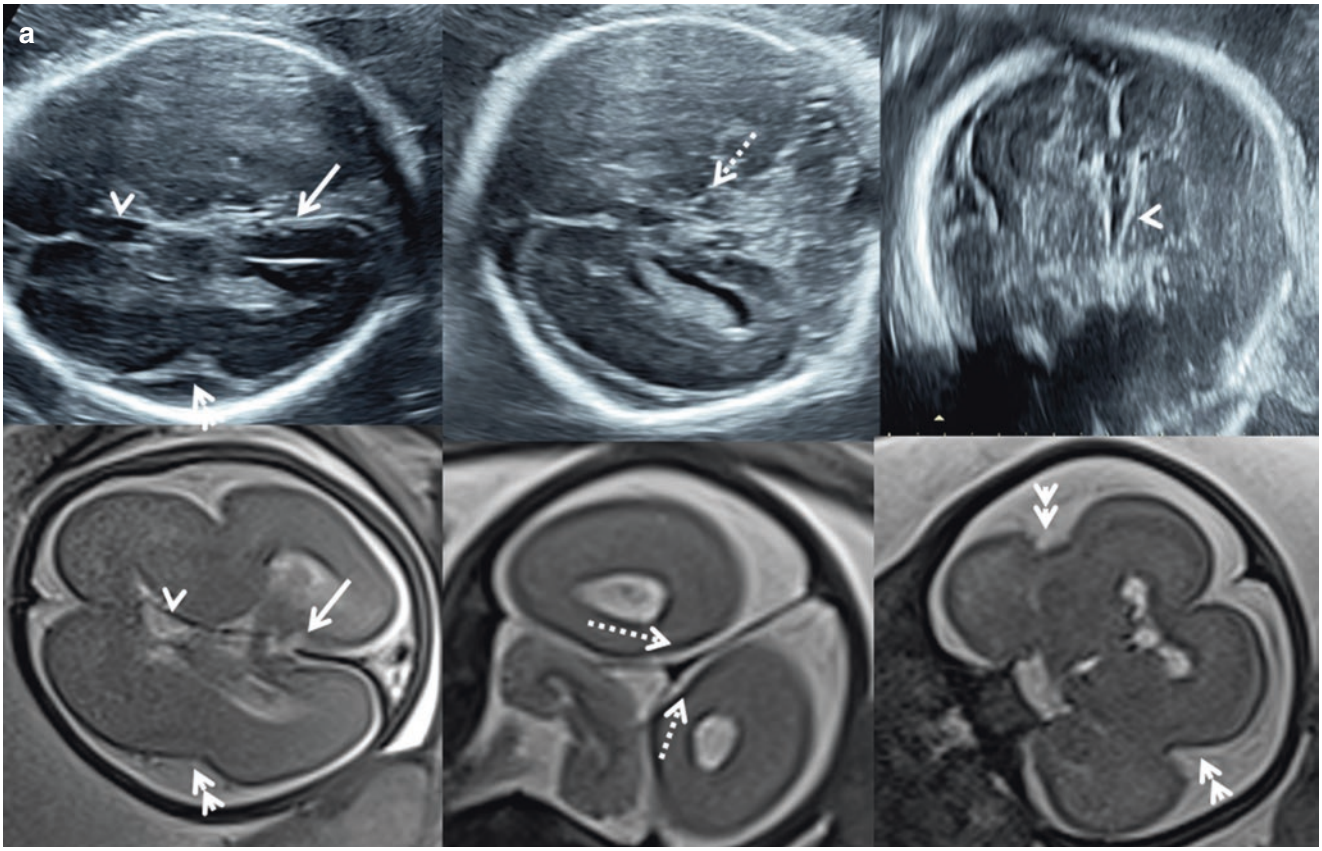

Fig. 4.8 (**a**) 28 weeks (TAS and MRI) *classical lissencephaly due to LIS1 (PAFAH1B1) gene mutation* – axial transventricular and transcerebellar and coronal transcaudate US and T2W sections – lateral ventricles are normal, CSP appears narrow (arrowheads), parieto-occipital (solid arrow) and calcarine (dotted arrow) sulci are barely visualised, lateral fissure (double arrowheads) is shallow and obtuse angled. Amniocentesis and clinical exome sequencing were done. (**b**) 28 weeks (TAS and MRI) *classical lissencephaly due to LIS1 (PAFAH1B1) autosomal dominant gene mutation* – mid- and parasagittal US and T2W MR sections – CC is normal (solid arrow), cerebral convexity sulci are not seen (dotted arrow), cingulate sulcus is not seen. The genetic report is shown

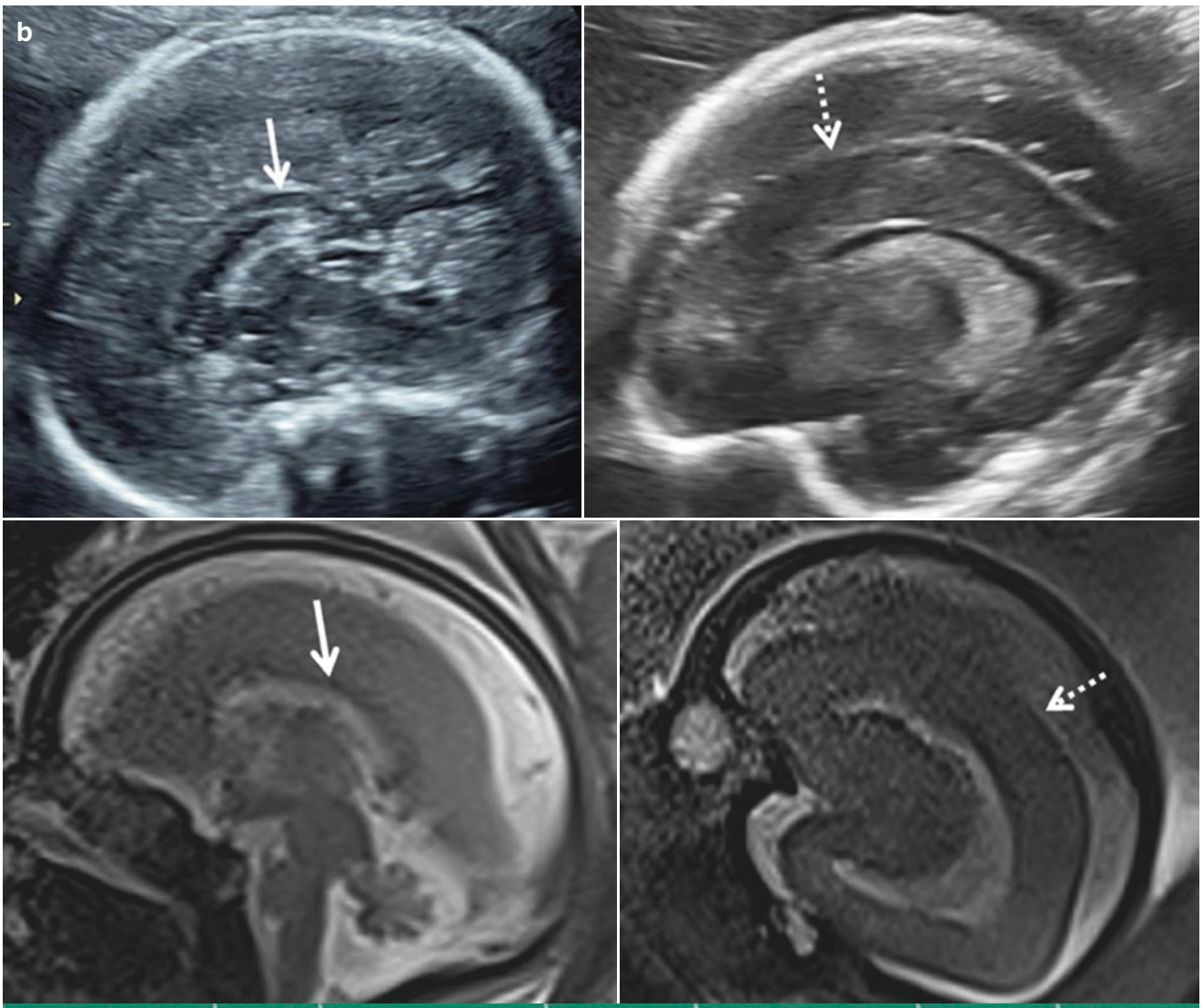

Gene (Transcript) #	Location	Variant	Zygosity	Disease (OMIM)	Inheritance	Classification
PAFAH1B1 **(+)** (ENST00000397195)	Exon 6	c.441dupA **(p.Gly148ArgfsTer28)**	Heterozygous	Lissencephaly 1, Subcortical laminar heterotopia	Autosomal dominant	Pathogenic

Fig. 4.8 (continued)

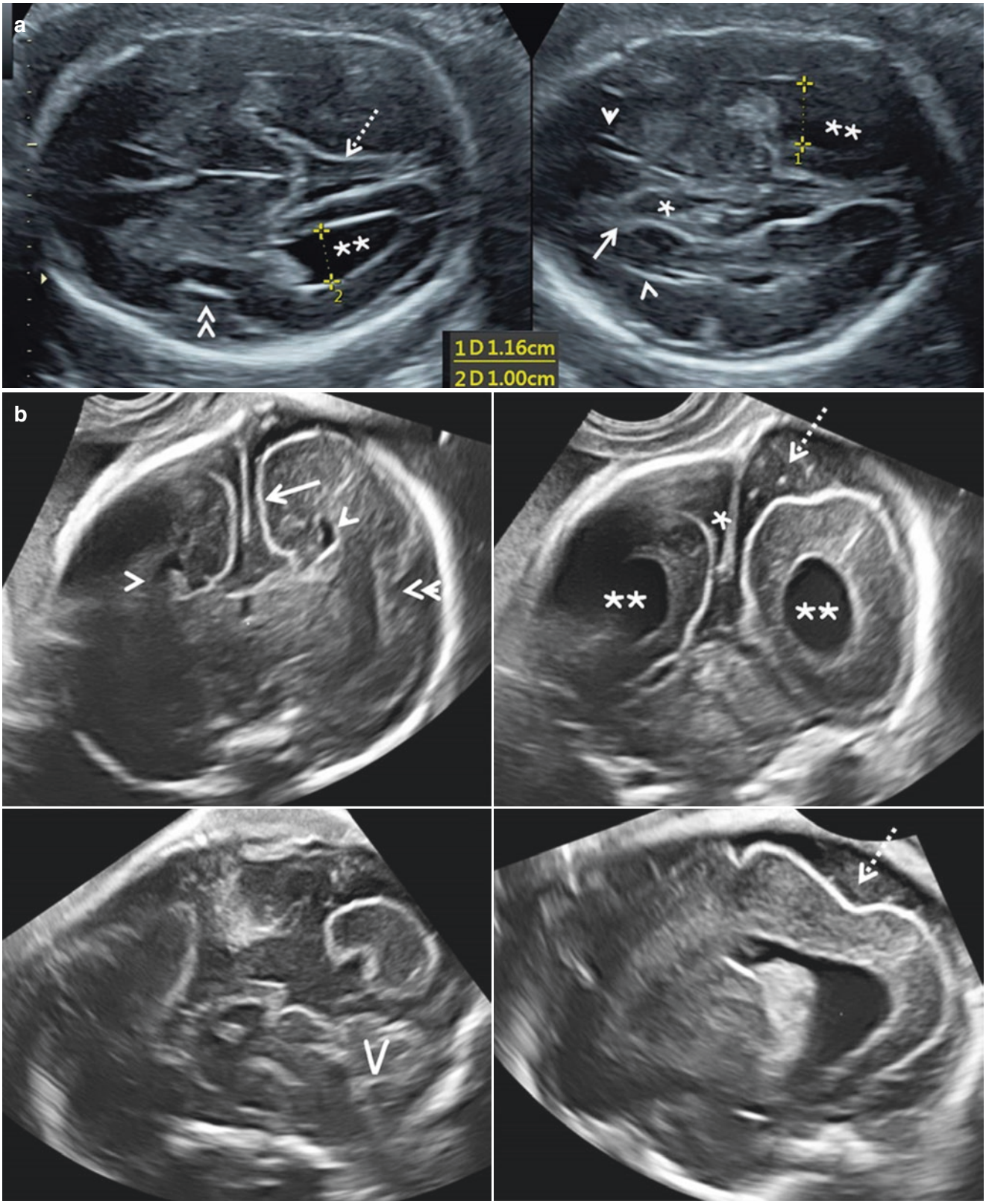

Fig. 4.9 (**a**) 27 weeks (TAS and TVS) *classical lissencephaly with complete agenesis of corpus callosum* – axial transventricular and slightly superior sections – mild bilateral lateral ventriculomegaly (**), laterally placed pinched anterior horns (arrowheads), wide IHF (*), shallow right angle-shaped lateral fissure (double arrowhead), parieto-occipital sulcus not seen (dotted arrow), cingulate sulcus not seen (solid arrow). Note CSP is not seen. (**b**) 27 weeks (TAS and TVS 3D multiplanar) *classical lissencephaly with complete agenesis of corpus callosum* – coronal transthalamic and transcerebellar sections, midsagittal and parasagittal sections – mild bilateral lateral ventriculomegaly (**), laterally placed 'steerhorn'-shaped anterior horns (arrowheads), wide IHF (*), shallow right angle-shaped lateral fissure (double arrowhead), cingulate sulcus not seen (solid arrow), corpus callosum is absent, vermis (V) well seen, increased subarachnoid space (dotted arrow)

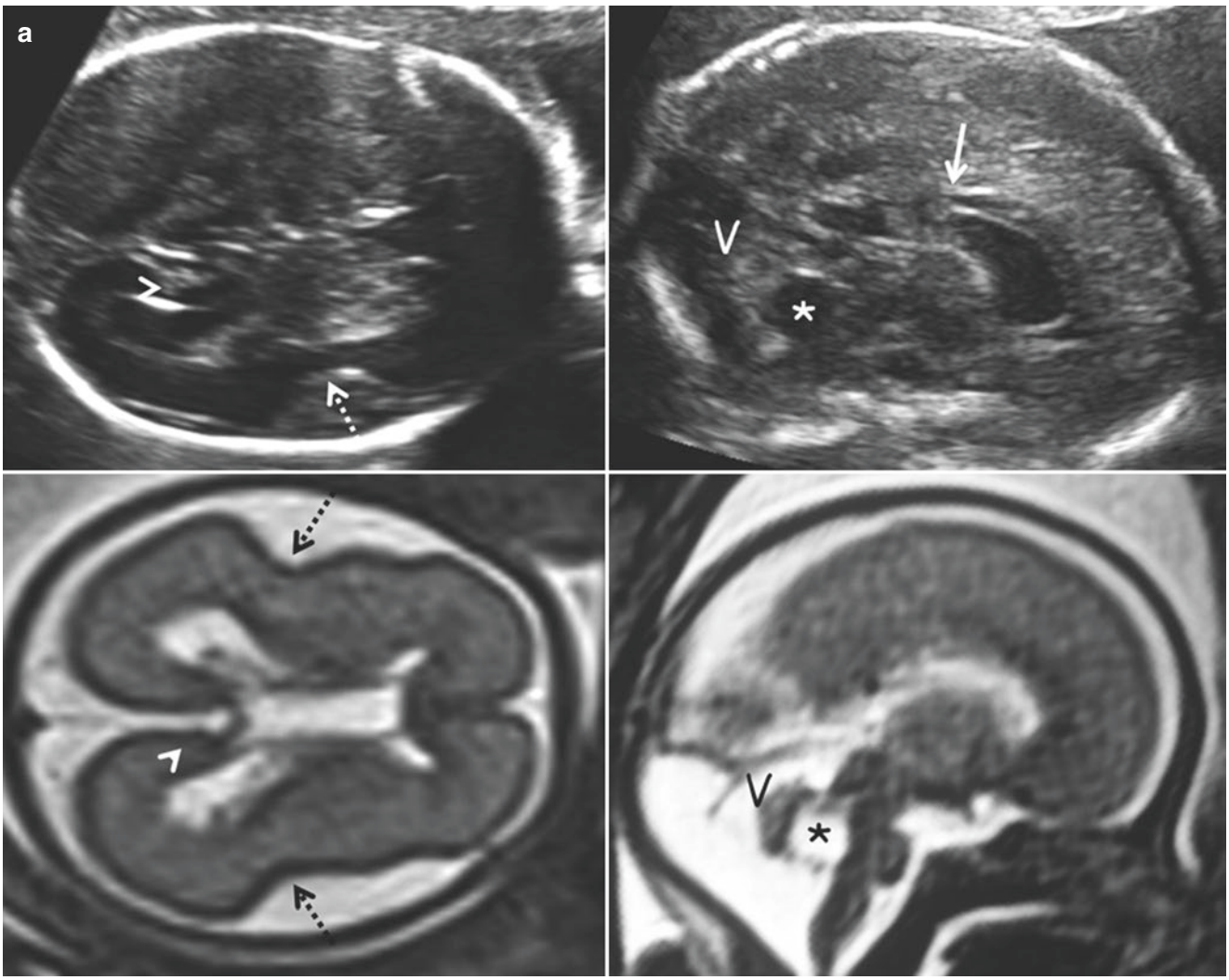

Fig. 4.10 (**a**) 25 weeks (TAS and MRI) *lissencephaly with partial agenesis of corpus callosum, dilated cystic fourth ventricle, sinus pericranii and persistent primitive falcine vein* – transventricular and midsagittal US and T2W sections – shallow parieto-occipital sulcus (arrowheads) and obtuse-angled lateral fissure (dotted arrows), splenium of CC is absent, posterior limit of CC (solid arrow) does not overlie the tectal plate, dilated fourth ventricle (*), the vermis is posteriorly displaced (V), its size is normal (cephalocaudal dimension of 1.3 cm and AP dimension of 0.8 mm). (**b**) 25 weeks (TAS and MRI) *lissencephaly with partial agenesis of corpus callosum, dilated cystic fourth ventricle, sinus pericranii and persistent primitive falcine vein* – slightly off-centre midsagittal sections B mode and color Doppler, T2W midsagittal section with magnification – small scalp cystic lesion overlying the posterior fontanelle is the sinus pericranii (solid arrows), persistent primitive falcine vein (dotted arrows) extending to the sinus pericranii

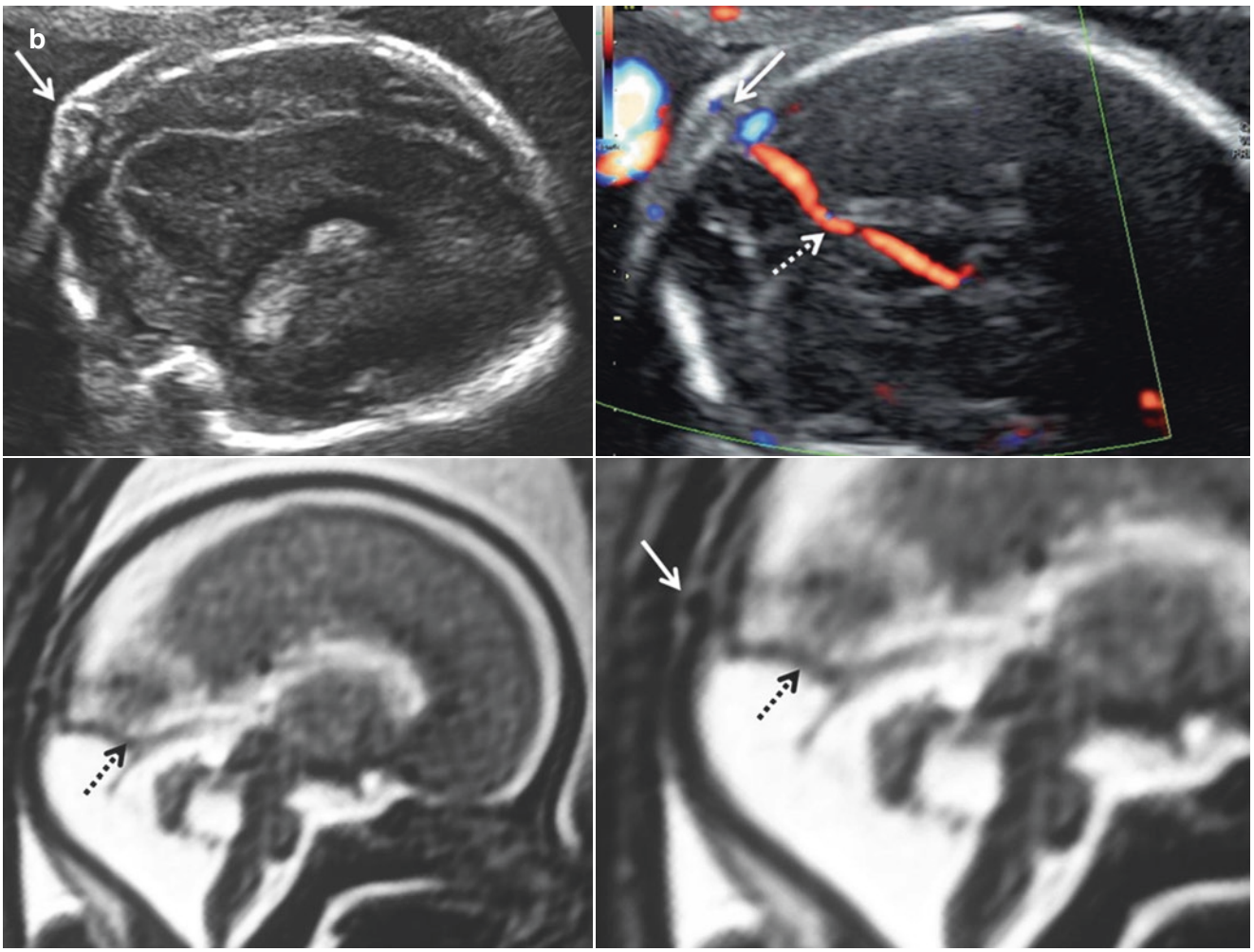

Fig. 4.10 (continued)

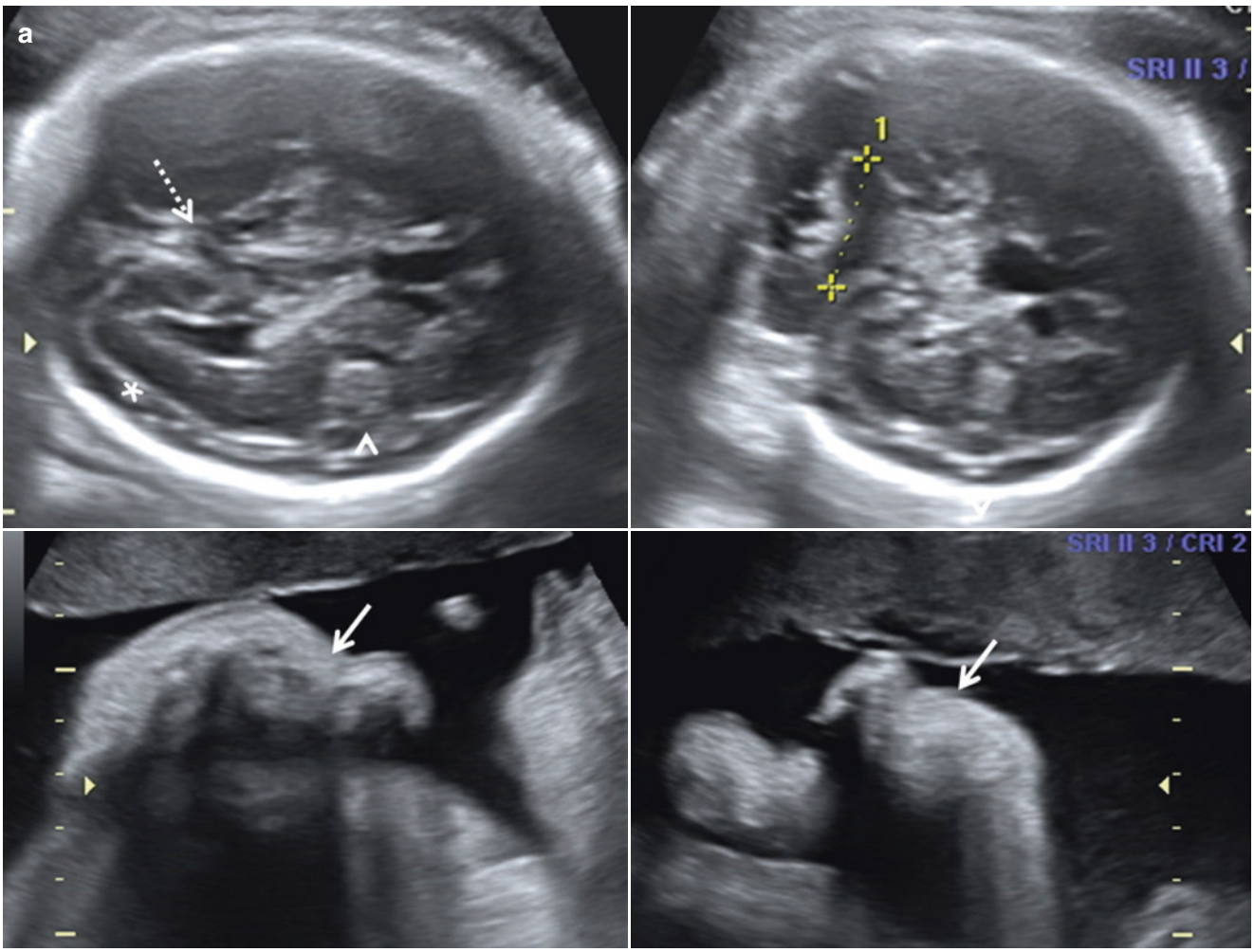

Fig. 4.11 (**a**) 26 weeks (TAS and MRI) *classical lissencephaly with cerebellar hypoplasia* – axial transventricular and transcerebellar sections, right and left hands – prominent subarachnoid space (*), shallow obtuse angle-shaped lateral fissure (arrowhead), parieto-occipital sulcus is barely seen (dotted arrow), cerebellar hypoplasia (TCD < fifth centile), bilateral hand joint contractures (solid arrows). Fetal tonic-clonic movements were seen. (**b**) 26 weeks (TAS and MRI) *classical lissencephaly with cerebellar hypoplasia* – axial transventricular, parasagittal and coronal transcaudate and transcerebellar sections – prominent subarachnoid space (*), shallow obtuse angle-shaped lateral fissure (arrowheads), parieto-occipital sulcus (dotted arrow) and convexity sulci not seen (solid arrow), cerebellar hypoplasia (TCD < 5^{th} centile)

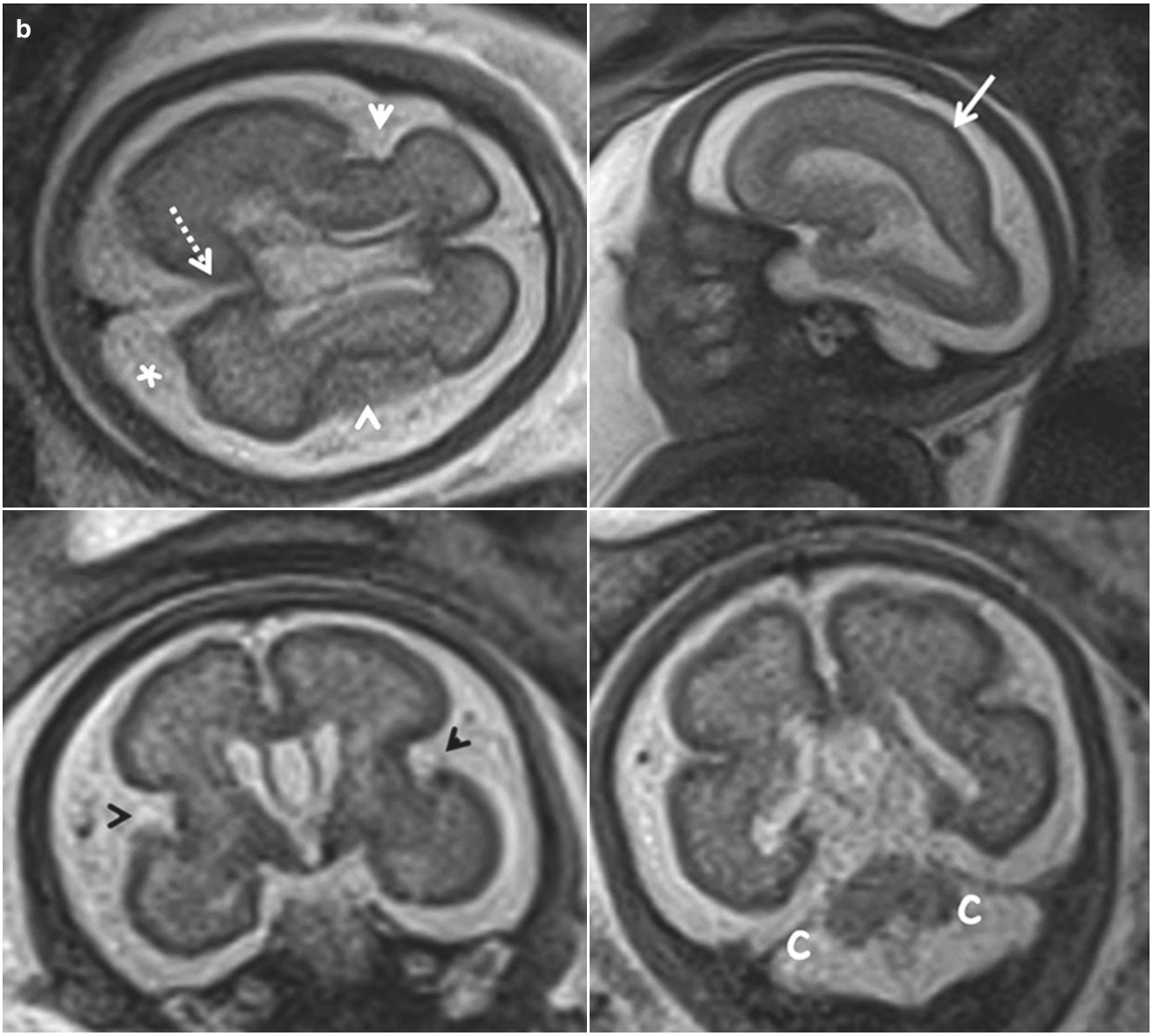

Fig. 4.11 (continued)

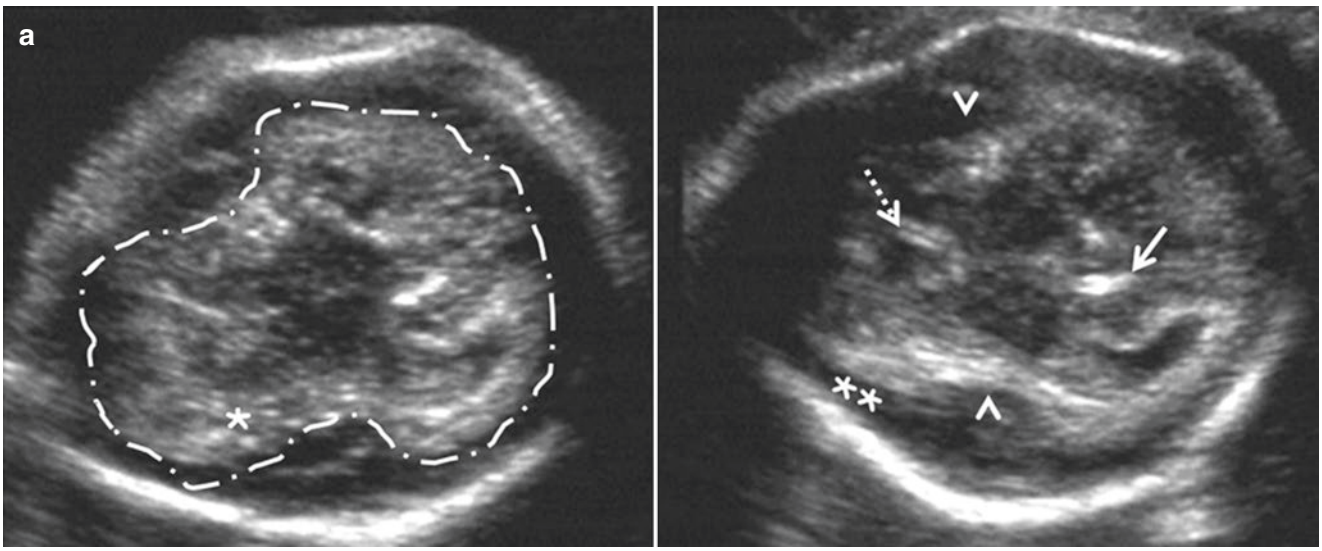

Fig. 4.12 (**a**) 26 weeks (TAS) *Miller-Dieker syndrome*, *classical lissencephaly with facial dysmorphism* – axial transventricular sections – thin hyperechoic cerebral parenchyma (*), increased subarachnoid space (**), shallow, obtuse-angled lateral fissure (arrowhead), parieto-occipital sulcus not seen (solid arrow), CSP is small (dotted arrow), figure of eight contour of the cerebrum (dot and dash outline). (**b**) 26 weeks (TAS) *Miller-Dieker syndrome, classical lissencephaly with facial dysmorphism* – axial section of orbits, midsagittal facial profile sections, coronal section of face, pictures of face of the abortus – prominent orbits, hypertelorism (interorbital distance more than 95th percentile) (double-headed arrow), small nose (dotted arrow), macroglossia (arrowhead), increased prenasal thickness (double arrowheads), arched upper lip (solid arrow). Picture of the abortus confirms all US findings. Echogenic intracardiac focus and polyhydramnios were also present

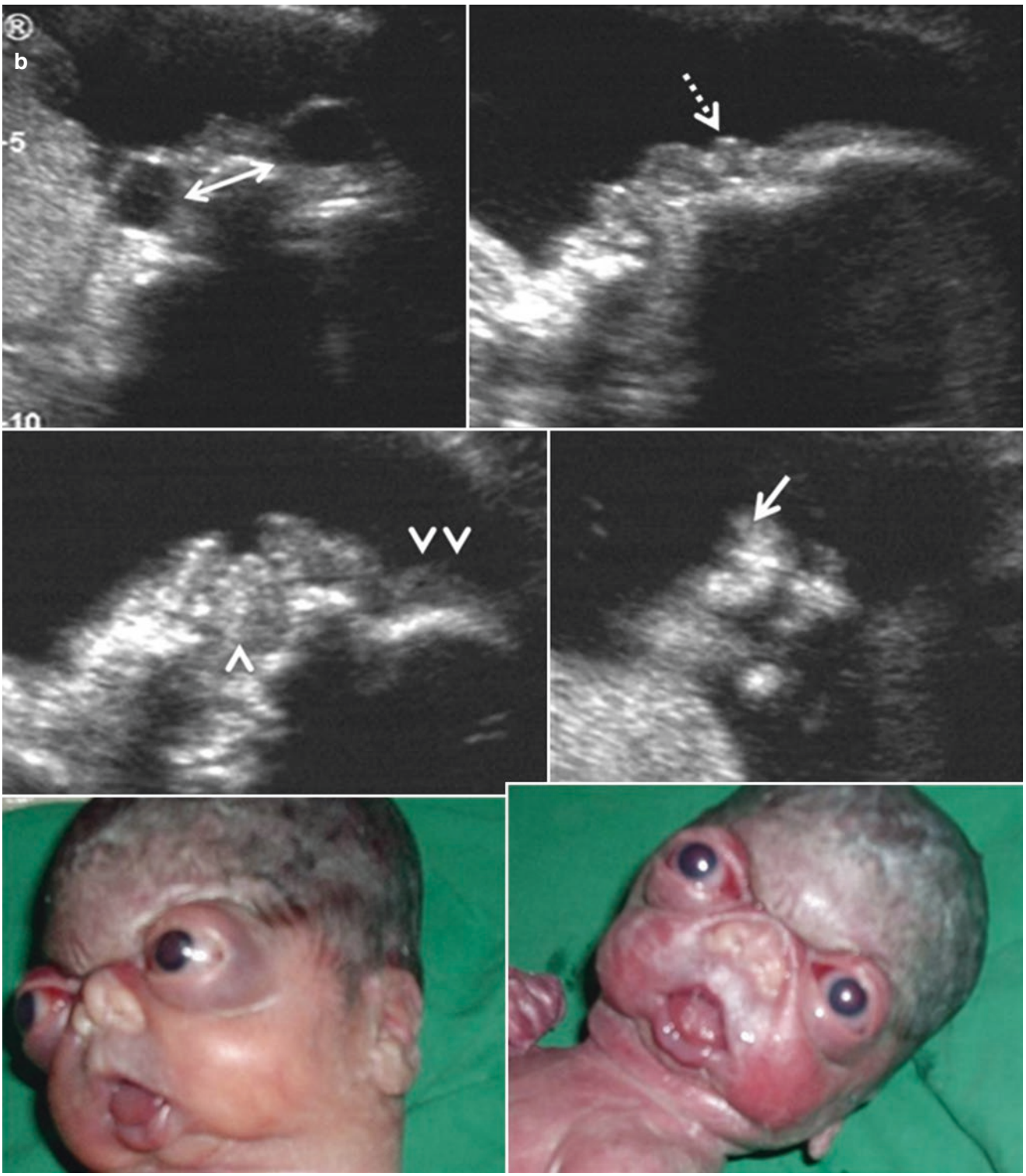

Fig. 4.12 (continued)

4.2.2 Cobblestone Complex

The radial neuronal migration is normally limited by the pia. In cobblestone complex (type II lissencephaly), there is radial over-migration of the neurons, resulting in neuroglial transgression of the pia and extension into the subarachnoid space. The abnormal migration results in an agyric brain covered by an extracortical neuroglial layer with a fine nodular surface. Cobblestone complex occurs in a group of autosomal recessive disorders termed the cobblestone complex syndromes. In the ascending order of severity, these are Fukuyama congenital muscular dystrophy, muscle eye brain disease and Walker-Warburg syndrome (WWS). Cobblestone complex, muscular dystrophy and ocular abnormalities are characteristic of these syndromes. WWS is the commonest in the group and is also known by the acronym HARD+/−E syndrome (*h*ydrocephalus, *a*gyria *r*etinal *d*ysplasia with or without *e*ncephalocele). WWS is caused by mutations in the POMT1, POMT2, POMTGNT1, FCMD, FKRP and LARGE genes (α-dystroglycanopathy genes).

The following are the intracranial findings in Walker-Warburg syndrome (cobblestone complex):

1. Hyperechoic layer of the abnormal extracortical neuroglia may be seen around the cerebral hemispheres. The presence of the neuroglial layer can also be seen in the basal cisterns as a hyperechoic region around the brainstem. The layer is not well seen on MRI (Fig. 4.13a–d).
2. The neuroglial layer obliterates the subarachnoid space around the cerebral hemispheres (Figs. 4.13b–d, 4.15a and 4.16a). Medially the cerebral hemispheres appear to be continuous with each other across the midline (pseudofusion) (Fig. 4.13a–d). This sign can be seen on ultrasonography and MRI. Hydrocephalus may also contribute to obliteration of the subarachnoid space.
3. Delayed (delay of three weeks or more) or absent sulcation can be detected (Figs. 4.13a–d, 4.14, 4.15a and 4.16a).
4. Frank lateral ventriculomegaly (atrial diameter more than 15 mm) and dilatation of the third ventricle indicate hydrocephalus (Figs. 4.13a, d and 4.16a). Hydrocephalus

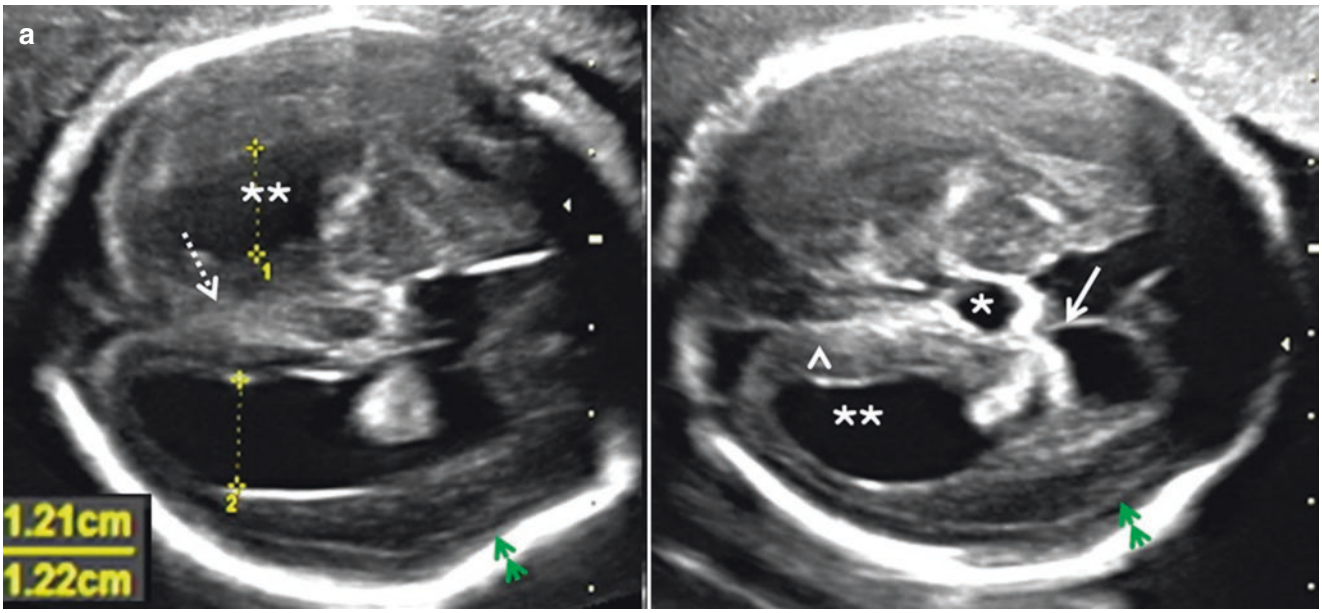

Fig. 4.13 (**a**) 25 weeks (TAS) *Walker-Warburg syndrome (cobblestone complex)* – axial transventricular sections – bilateral mild ventriculomegaly (**), no fluid between the layers of the septum pellucidum (solid arrow), third ventricle is prominent (*), parieto-occipital sulcus (arrowhead) and lateral fissure (double arrowheads) are not seen, posterior interhemispheric fissure is obliterated with pseudofusion of the occipital lobes across the midline (dotted arrow), no occipital encephalocele was noted. (**b**) 25 weeks (TAS) *Walker-Warburg syndrome (cobblestone complex)* – oblique axial transventricular and parasagittal sections – mild lateral ventriculomegaly (**) with dysmorphic shape, pericerebral hyperechoic layer in the occipital (single arrowhead) and cerebral convexity (solid arrows) regions, pseudofusion of the occipital lobes across the midline (dotted arrow). (**c**) 25 weeks (TAS 3D US) *Walker-Warburg syndrome (cobblestone complex)* – multiplanar transventricular axial, rendered axial transventricular, multiplanar midsagittal and multiplanar midbrain axial sections – hyperechoic band around the occipital lobes with finely irregular cerebral surface (double arrowheads), occipital lobe pseudofusion across the midline (arrowhead), CC thin towards the splenium (*), Z-shaped, kinked brainstem (dotted line), hyperechoic region seen anterior and posterior to the brainstem and around the midbrain in the quadrigeminal, ambient and interpeduncular cisterns (dotted arrows). (**d**) 25 weeks (MRI) *Walker-Warburg syndrome (cobblestone complex)* – T2W MR axial section cephalad to the transventricular plane, axial transventricular and transthalamic, coronal transfrontal and transcerebellar and midsagittal sections – bilateral lateral ventriculomegaly (**), frontal lobe pseudofusion across the midline (white solid arrow), parieto-occipital (small arrowhead) and lateral fissures (double arrowheads) are not seen, occipital lobe pseudofusion across midline (black solid arrow), loss of pericerebral space (large arrowhead), Z-shaped, kinked brainstem (dotted arrow), thin splenium of CC (*). (**e**) 25 weeks (TAS and MRI) *Walker-Warburg syndrome (cobblestone complex)* – axial, coronal and sagittal US and T2W sections of the orbits – thick dysplastic retina is anchored centrally to the optic disc (arrowhead), and its anterior edge is circumferentially attached to the ora serrata (solid arrow), circumferentially nonattached retina on coronal section (dotted arrow)

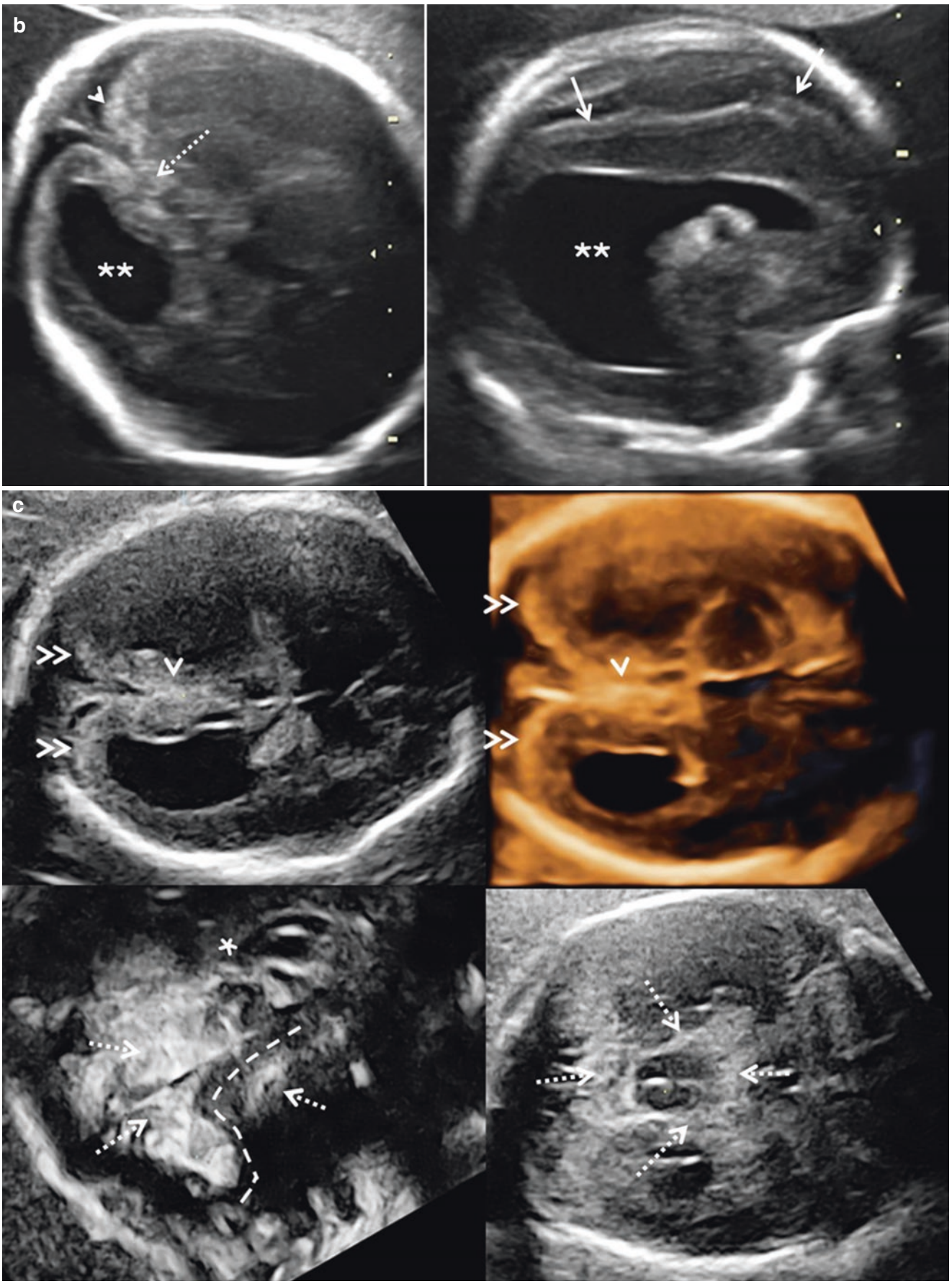

Fig. 4.13 (continued)

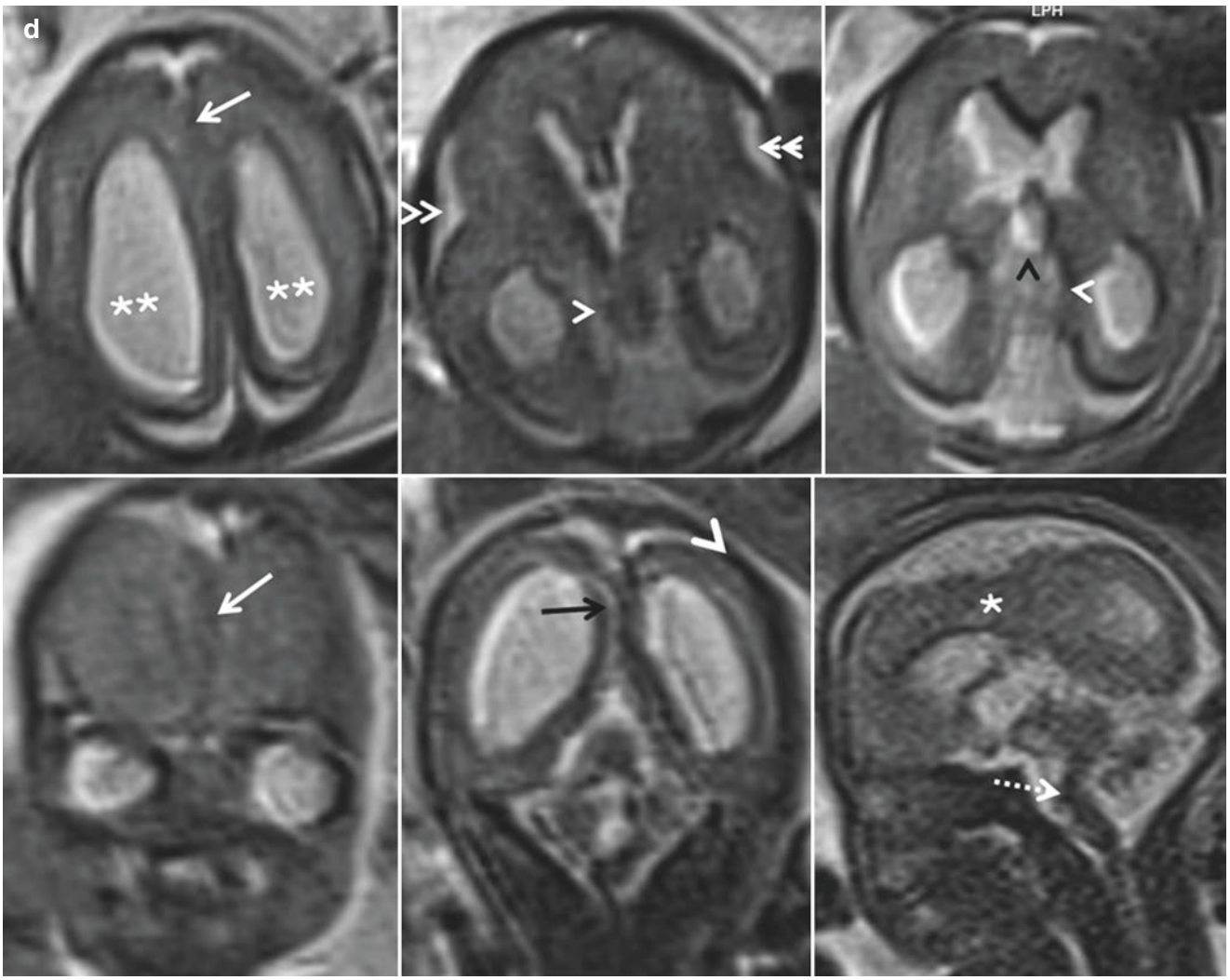

Fig. 4.13 (continued)

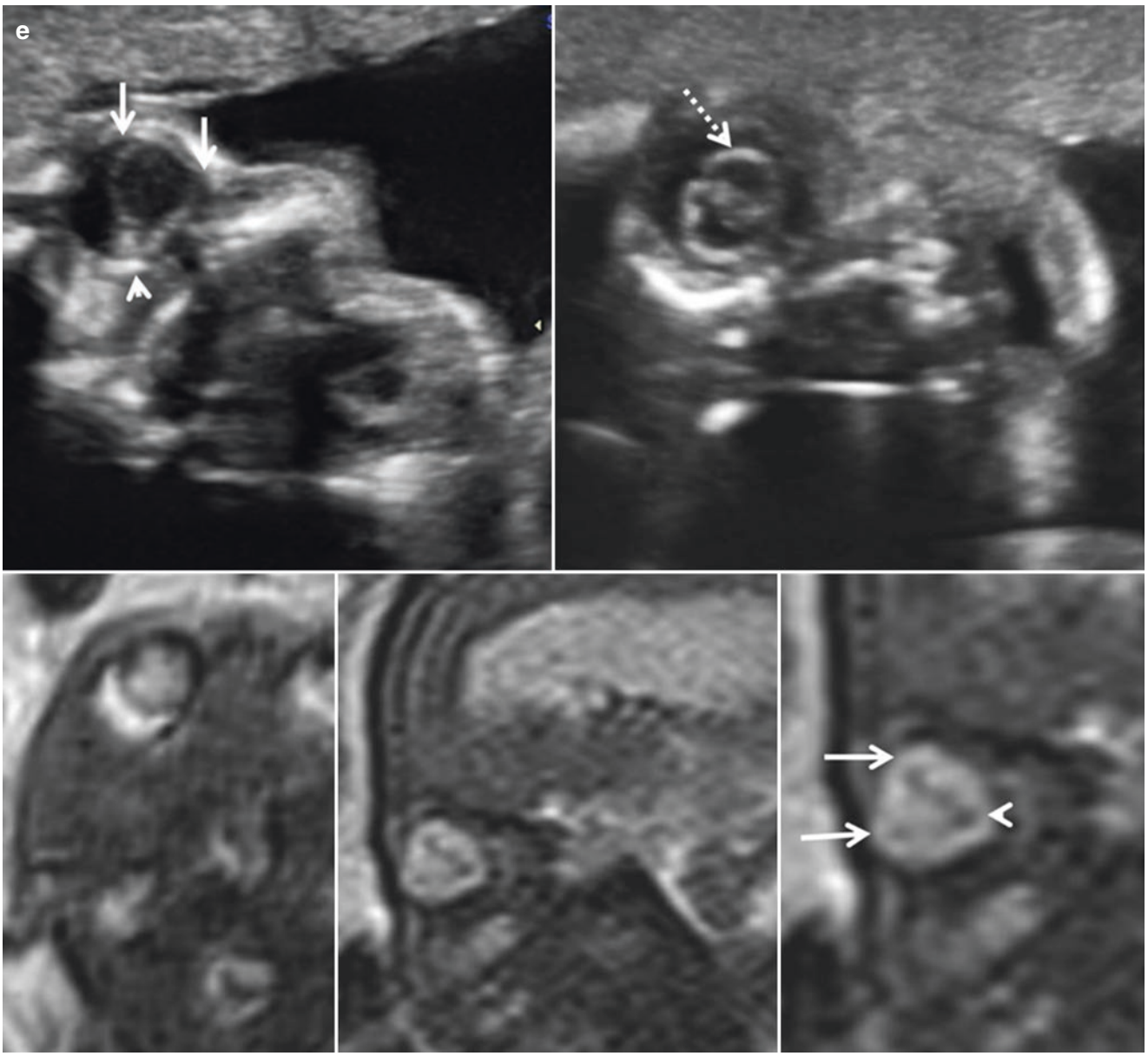

Fig. 4.13 (continued)

may be due to choking of the subarachnoid space around the cerebral convexity by the leptomeningeal thickening, preventing access of CSF to the arachnoid villi (Pacchionian bodies).

5. Occipital encephalocele may be seen (Fig. 4.14).
6. Z-shaped or kinked brainstem, seen in the midsagittal section, is due to persistence of the embryonic pontine flexure (Fig. 4.13c, d). This finding may also be detected in the first trimester (11–14 weeks) US examination.
7. Vermian abnormalities may range from subtle vermian hypoplasia to frank Dandy-Walker malformation Figs. 4.15a and 4.16a).

The following are the extracranial abnormalities in Walker-Warburg syndrome:

1. Ocular abnormalities include microphthalmia, buphthalmos (large size of the globe), cataract, retinal dysplasia (thickening) and retinal non-attachment. The non-attached retina typically assumes a funnel shape as its margin and centre are attached to the ora serrata and optic disc, respectively (Figs. 4.13e, 4.14, 4.15a, b and 4.16b).
2. Other associated abnormalities such as micropenis, cryptorchidism, cleft lip and palate and low-set ears may be present.

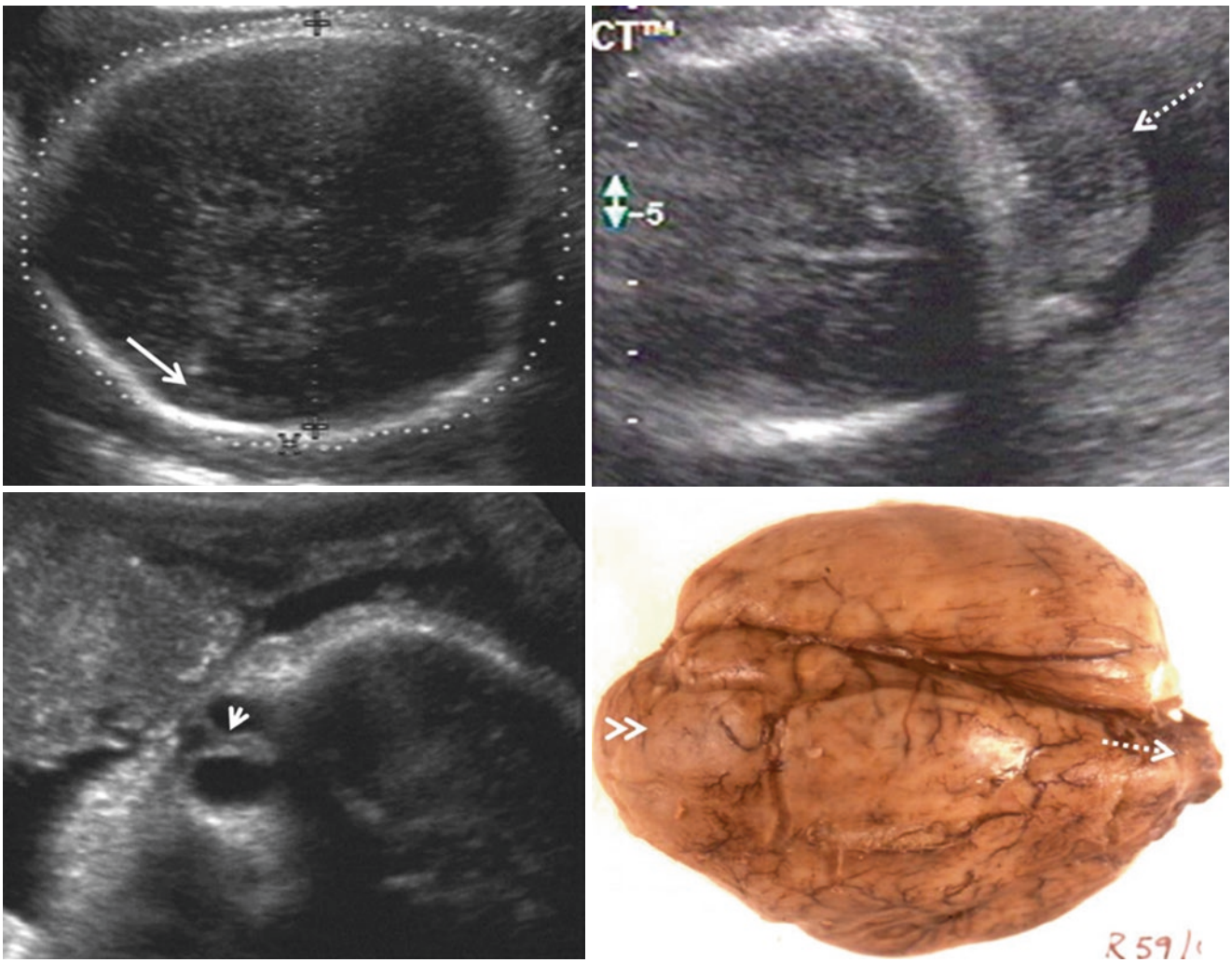

Fig. 4.14 35 weeks (TAS) *Walker-Warburg syndrome with occipital encephalocele (cobblestone complex)* – axial sections of cranium, parasagittal orbital section and autopsy picture of the fetal brain – microcephaly, no convexity sulcation (solid arrow), occipital encephalocele (dotted arrow), non-attached thick dysplastic retina (arrowhead), coarse cobbled cerebral surface (double arrowheads)

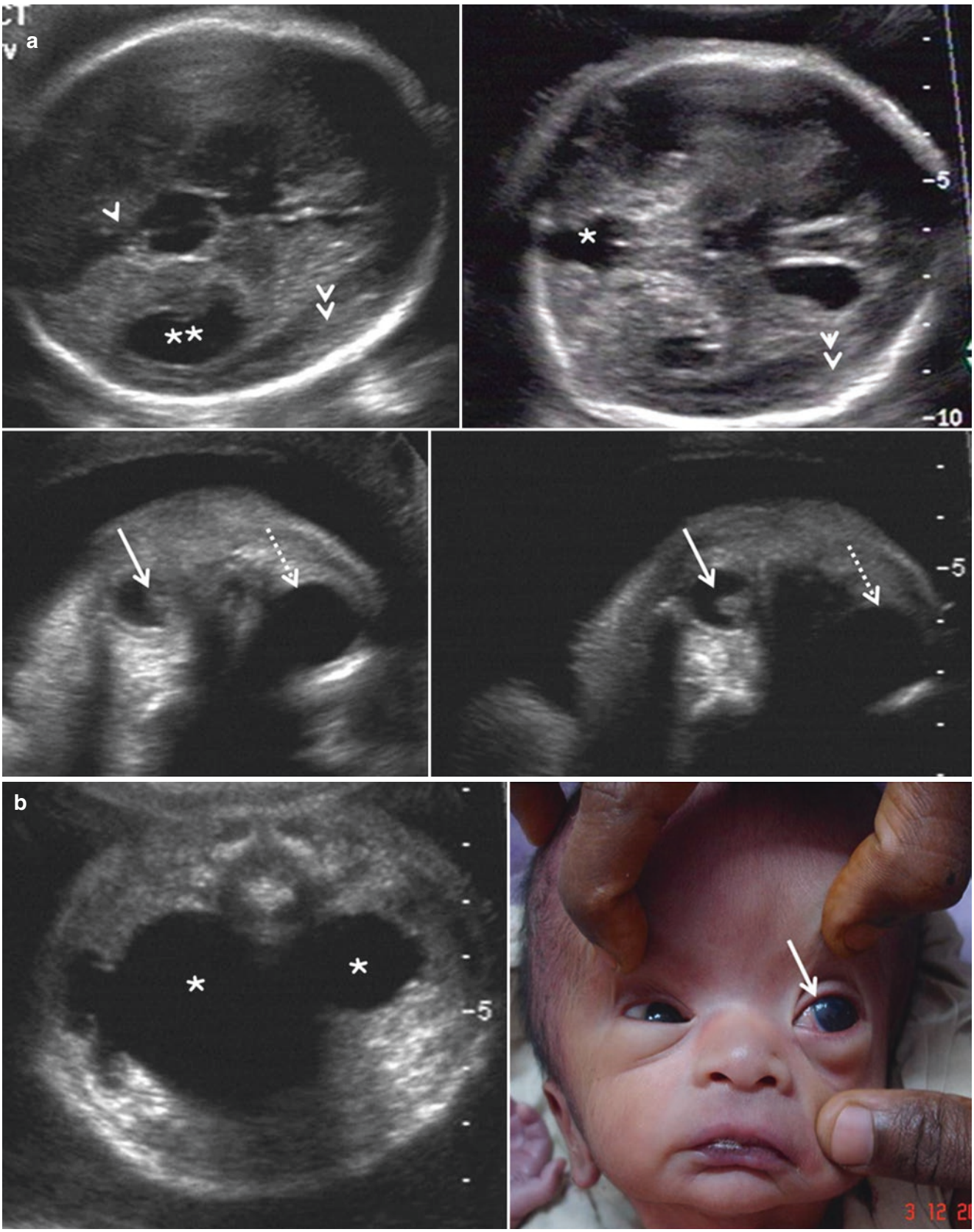

Fig. 4.15 (**a**) 31 weeks (TAS) *Walker-Warburg syndrome (cobblestone complex)* – axial transventricular and transcerebellar sections and axial sections of orbit – bilateral lateral ventriculomegaly (**), parieto-occipital sulcus (arrowhead) and lateral fissure (double arrowheads) not seen, obliteration of cerebral convexity subarachnoid space, open fourth ventricle (*), right orbit is small with a nubbin of thick non-attached retina (solid arrow), left orbit is large (megalophthalmos) due to buphthalmos (dotted arrow). (**b**) 31 weeks (TAS) *Walker-Warburg syndrome (cobblestone complex)* – axial section of the abdomen and postnatal picture of face – bilateral pelviureteric junction obstruction (*), larger left eye with megalocornea (solid arrow)

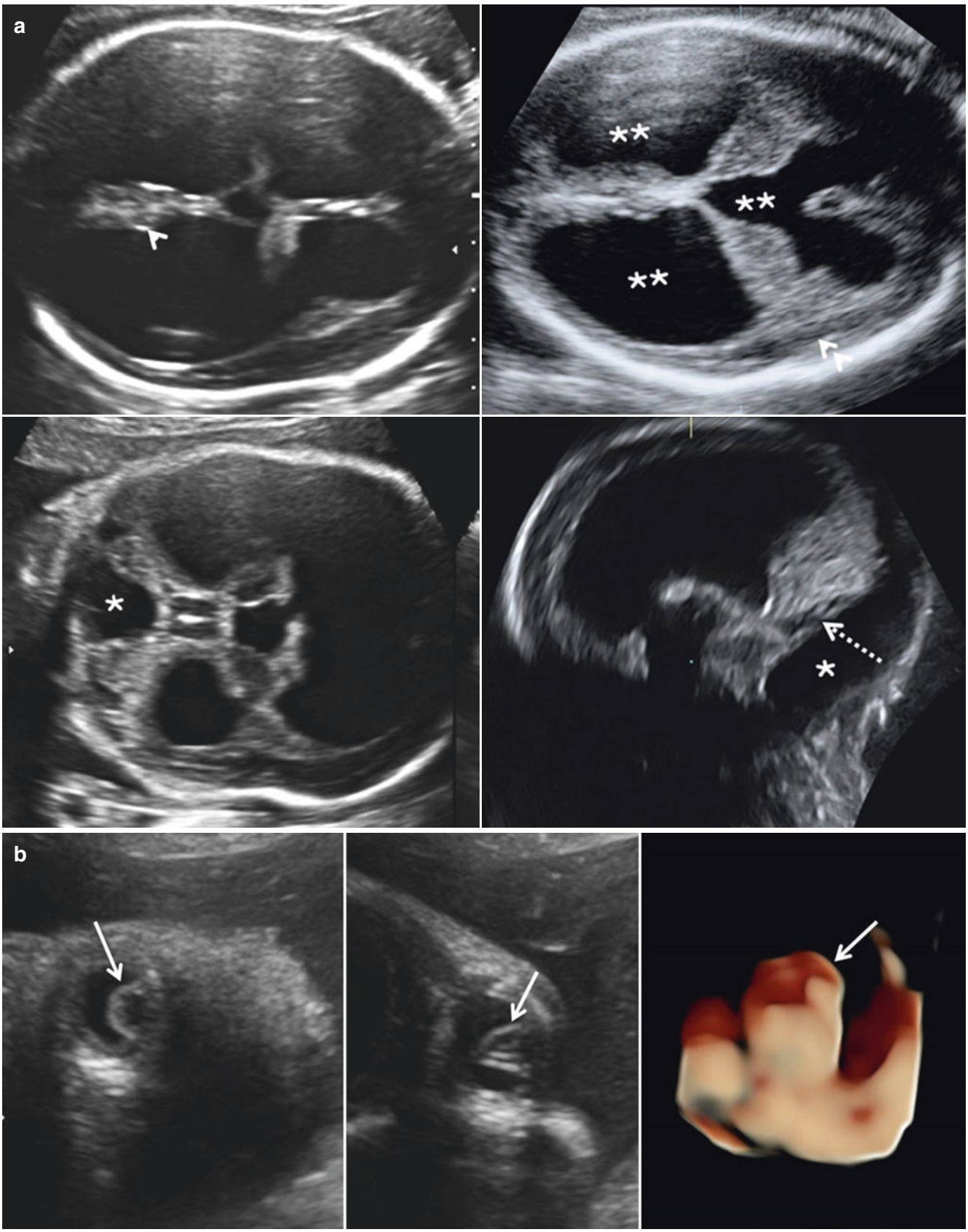

Fig. 4.16 (**a**) 30 weeks (TAS) *Walker-Warburg syndrome with Dandy-Walker malformation* – axial transventricular, transthalamic and transcerebellar sections and midsagittal section – bilateral lateral and third ventriculomegaly (**), parieto-occipital sulcus (arrowhead) and lateral fissure (double arrowhead) not seen with obliteration of the subarachnoid space, posterior cranial fossa cyst (*), compressed, deformed, elevated vermis (dotted arrow). (**b**) 30 weeks (TAS, 3D US) *Walker-Warburg syndrome with Dandy-Walker malformation* – coronal and axial sections of the right orbit and 3D surface rendering – thickened dysplastic non-attached retina anchored posteriorly to the optic disc. Its anterior edge is circumferentially attached to the ora serrata forming a cone (solid arrow)

Fetal MRI helps to confirm ultrasound findings and to obtain sections which were not optimal or possible with ultrasound.

4.2.3 Neuronal Heterotopia

The neuronal cell bodies are normally present only in the cortical grey matter and basal ganglia of the brain. Presence of clusters of neuronal cell bodies (grey matter) in an abnormal location (white matter) is termed heterotopia. Heterotopia is seen in the pathway of neuronal migration from the germinal matrix to the cortex.

There are two types of heterotopias, nodular and band. Nodular heterotopia is of the periventricular or subcortical types depending on the location of the nodules. Band heterotopia is subcortical. Bilateral periventricular nodular heterotopias (BPNH) can be recognised prenatally due to the abnormality in the margins of the lateral ventricles caused by the nodules. There are two genetic forms of BPNH with the same phenotypic end result. The X-linked recessive form is caused by a mutation in the filamin A gene (FLNA). In females it manifests as late onset epilepsy. Intellect is generally normal or mildly impaired. It is usually lethal in the embryonic period in males. In the few surviving males, there is severe neurological and intellectual disability. The autosomal recessive form is caused by mutations in the ARFGEF2 gene.

The ultrasound findings are as follows:

1. Bilateral bumpy lateral ventricular walls are seen. The contour or margin irregularity is better seen with high-frequency TAS and TVS examinations (Figs. 4.17a–c, 4.18 and 4.23a).
2. Small periventricular nodules of 2–3 mm size are seen almost isoechoic to the surrounding brain. The nodules can be recognised under the bump that it has produced on the lateral ventricular margin. They are best visualised in the magnified parasagittal or coronal sections. The nodules are multiple and either scattered or seen in a continuous array. A thin hyperechoic margin around each nodule may, sometimes, be noted (Figs. 4.17a–c and 4.23a, b).
3. Mild lateral ventriculomegaly is often the first abnormal finding to be detected (Figs. 4.17a–c and 4.18a, b).
4. Abnormal (square) shape of the lateral ventricles is best seen in the transcaudate and transthalamic coronal sections (Fig. 4.17a).
5. Bumpy relief of the lateral ventricular ependymal surface is well seen on 3D surface rendering of the lateral ventricles (Fig. 4.17b, 4.18 and 4.23f).
6. Pitted appearance of the lateral ventricular surface is seen by rendering in the inversion mode (Fig. 4.17b).
7. Associated findings are polymicrogyria, schizencephaly (Fig. 4.23a, b, f) or cerebellar hypoplasia.

Periventricular hemorrhage and tubers are to be differentiated from BPNH. Germinal matrix hemorrhage typically occurs at the caudothalamic groove, and its appearance changes with the age of the bleed. Associated intraventricular or parenchymal hemorrhage may be present. Subependymal or cortical tubers in tuberous sclerosis are larger and are faintly hyperechoic. Associated cardiac rhabdomyomas clinch the diagnosis.

Fetal MRI helps to confirm ultrasound findings and to detect associated intracranial abnormalities. The periventricular nodules are hypointense on T2 weighted images. Contrast resolution of MRI is better than that of ultrasound, whereas spatial resolution of the ultrasound (especially TVS) scores over MRI. This gives ultrasound an edge as the nodules are barely 2–3 mm in diameter. An irregular lateral ventricular margin seen on TAS should prompt a neurosonogram.

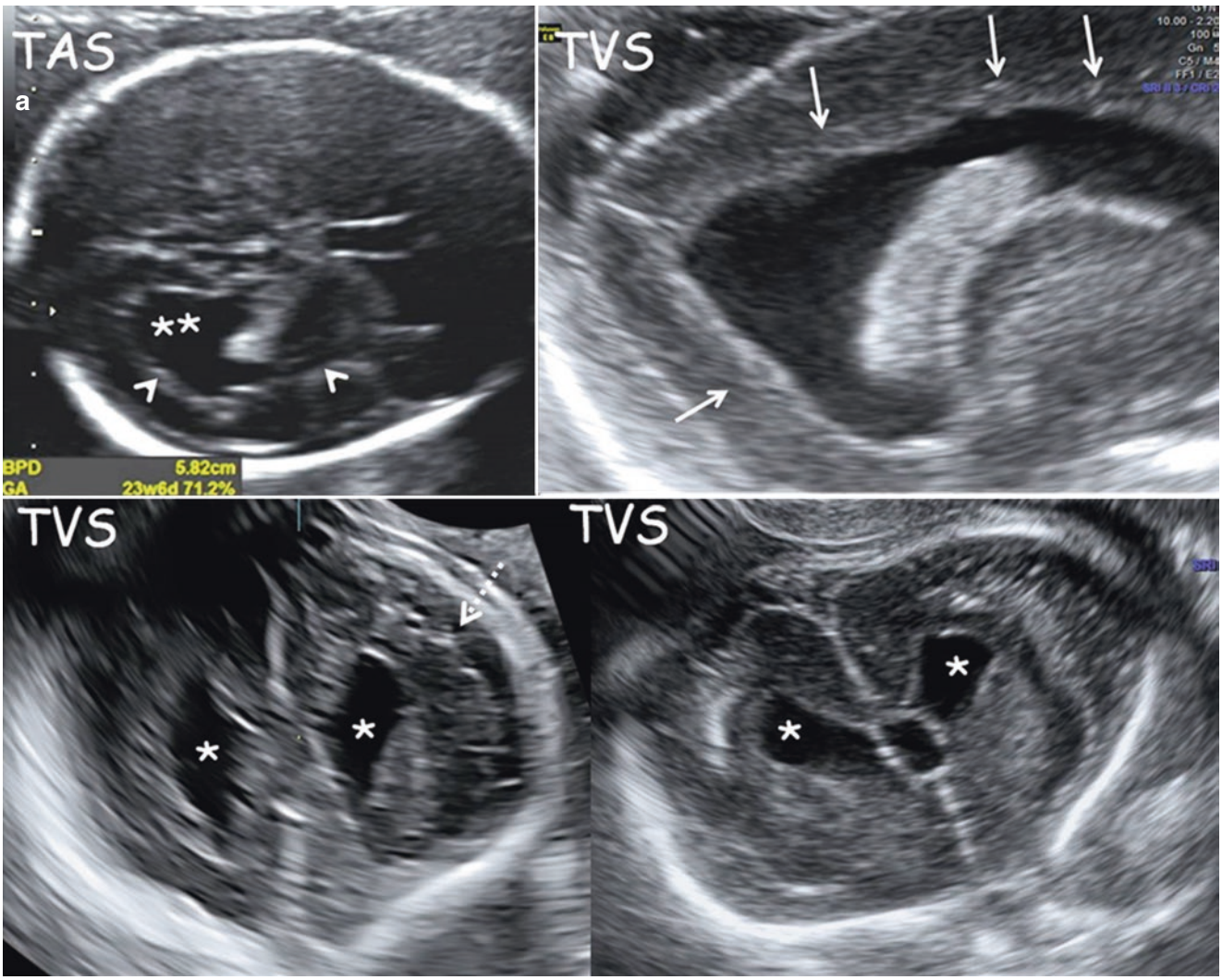

Fig. 4.17 (**a**) 23 weeks (TAS, TVS and MRI) *periventricular nodular heterotopia with polymicrogyria* – axial transventricular, parasagittal, coronal transfrontal and transcaudate sections – lateral ventriculomegaly (**), irregular bumpy lateral ventricular margin (arrowheads), periventricular nodules (solid arrows), dysmorphic square-shaped lateral ventricles (*), premature appearance of small convexity sulci and gyri (dotted arrow). (**b**) 23 weeks (TAS, TVS 3D US and MRI) *periventricular nodular heterotopia with polymicrogyria* – lateral ventricular surface rendering and inversion mode – irregular, bumpy internal relief of the lateral ventricle (solid arrows) and pitted surface on the inversion mode (dotted arrow). (**c**) 23 weeks (TAS, TVS and MRI) *periventricular nodular heterotopia with polymicrogyria* – axial transventricular and parasagittal, T2W sections – lateral ventriculomegaly (**), irregular bumpy lateral ventricular margin (arrowheads)

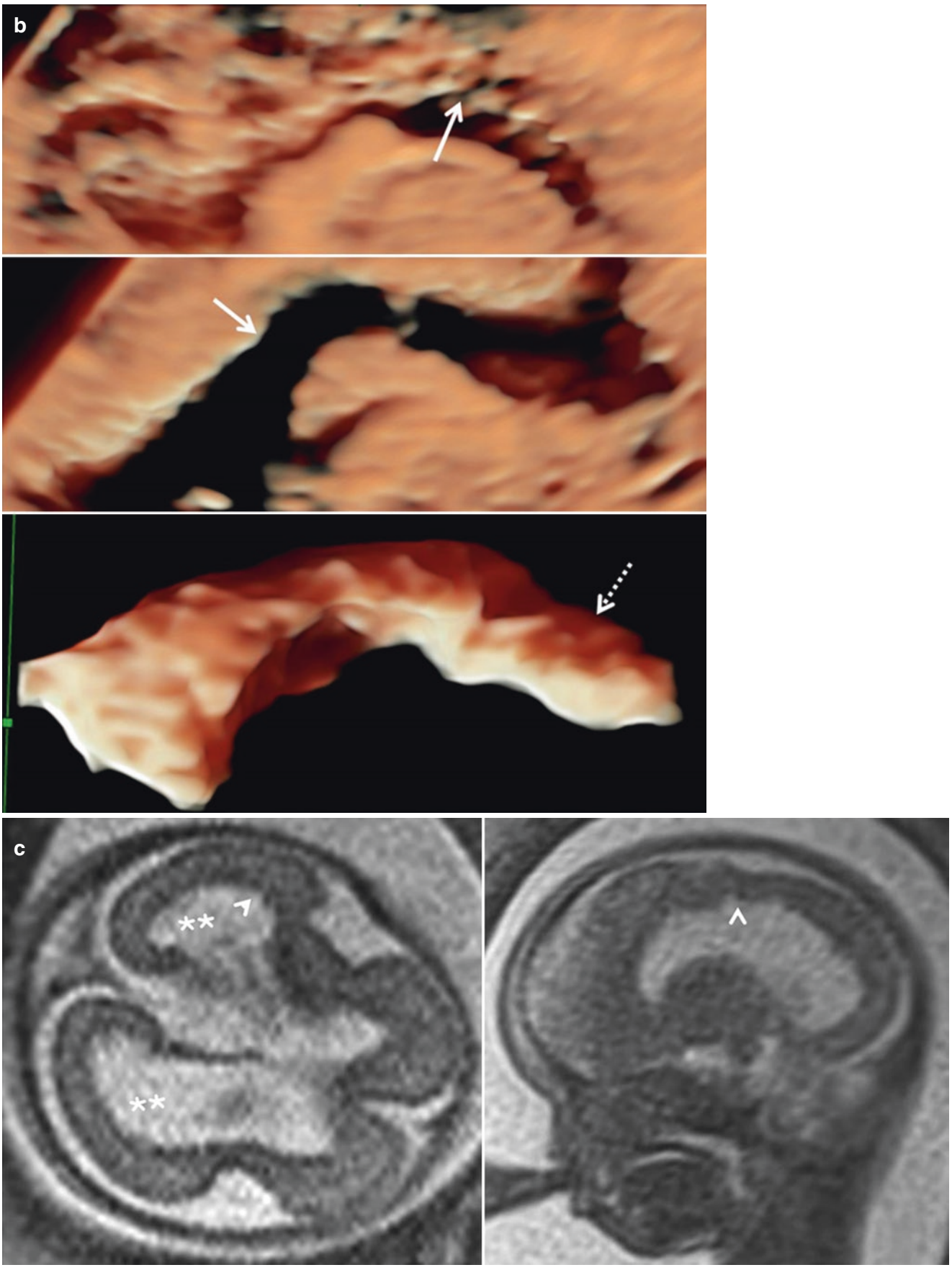

Fig. 4.17 (continued)

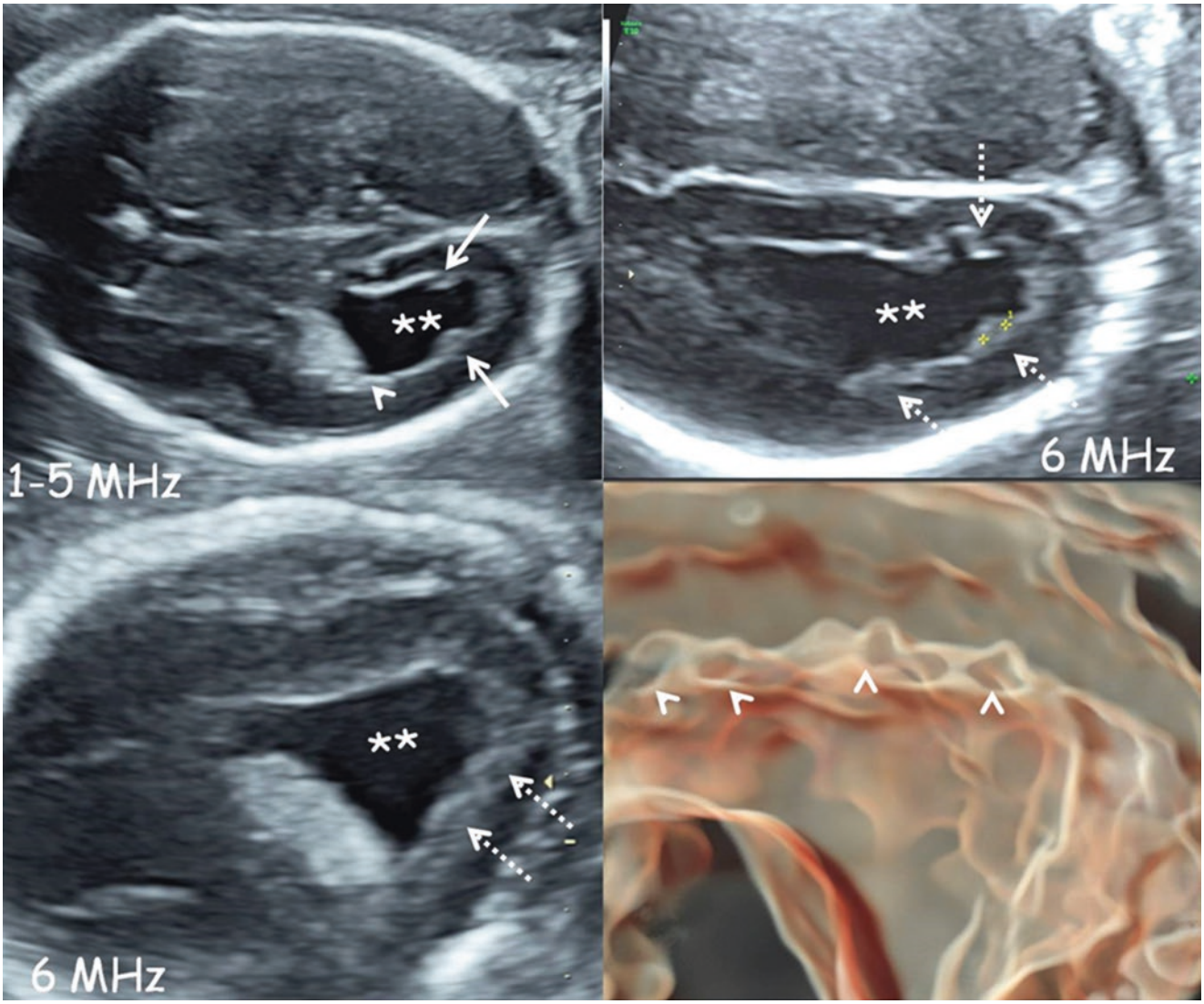

Fig. 4.18 21 weeks (TAS) *periventricular nodular heterotopia* – axial transventricular (1–5 MHz), transventricular axial (6 MHz), parasagittal (6 MHz) and 3D rendering with silhouette – lateral ventriculomegaly (**), irregular bumpy crinkled lateral ventricular margin (solid arrows) underlying nodules seen better with 6 MHz (dotted arrows), periventricular nodules are very well seen on 3D render mode with HD live and silhouette (arrowheads)

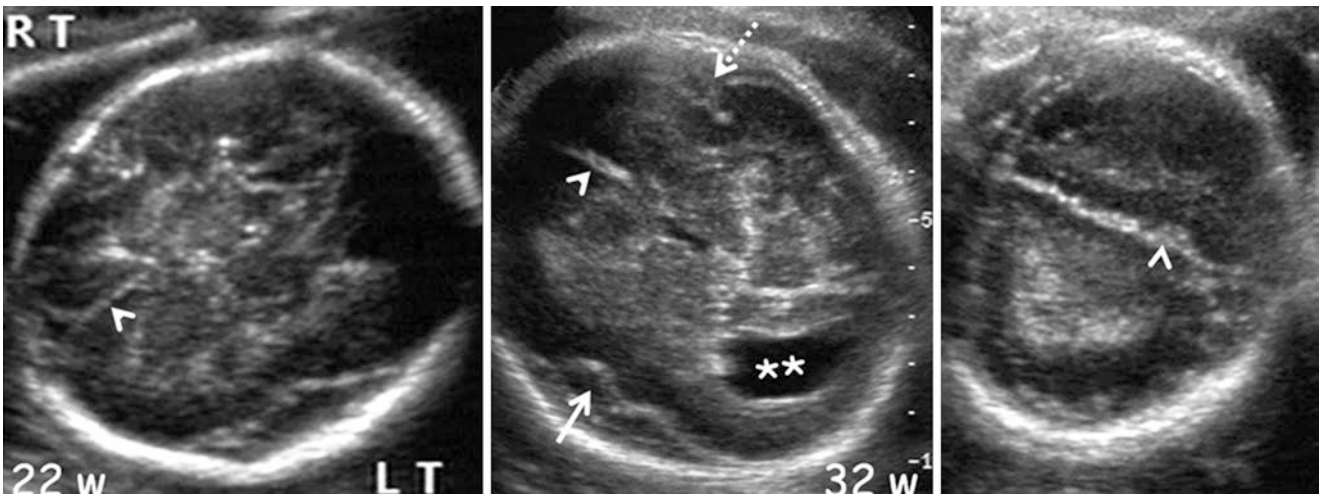

Fig. 4.19 22 and 32 weeks (TAS) *hemimegalencephaly* – axial transventricular and transfrontal coronal sections – left lateral ventriculomegaly (atrial dimension of 14 mm) (**), midline falx echoes (arrowheads) are shifted to the right due to the larger left cerebral hemisphere, delayed operculation of the left lateral fissure (solid arrows), appropriate operculation of right lateral fissure (dotted arrows)

4.2.4 Hemimegalencephaly

Unilateral cerebral hemispheric overgrowth with abnormalities in that hemisphere is characteristic of hemimegalencephaly. There is a midline shift to the contralateral side. The abnormalities of the larger hemisphere include ventriculomegaly, agyria, focal cortical dysplasia, white matter disease and calcification (Figs. 4.19 and 4.23a, b, g). It occurs either as an isolated finding or as a part of a syndrome such as Klippel-Trenaunay-Weber, Sotos, Proteus or linear nevus. Klippel-Trenaunay-Weber syndrome is characterised by multiple subcutaneous haemangiomas and localised soft tissue or bony hypertrophy in the limbs. Hemimegalencephaly manifests as intractable seizures, and hemispherectomy is the treatment of choice.

4.3 Disorders of Neuronal Organisation

This group includes tuberous sclerosis, schizencephaly and polymicrogyria. Although grouped under disorders of neuronal organisation, the pathogenesis of polymicrogyria may involve the phases of neuronal proliferation and migration.

4.3.1 Tuberous Sclerosis

Tuberous sclerosis is an autosomal dominant multisystem disorder caused by mutations in the TSC1 or TSC2 genes. These genes code for the proteins hamartin and tuberin which are tumor suppressors. Fetal cardiac rhabdomyomas and cerebral hamartomas (tubers) are the morphological findings which enable prenatal diagnosis. Cardiac rhabdomyomas appear late in the second or early third trimester and are often multiple. Seventy-five percent of fetuses with rhabdomyomas have tuberous sclerosis. Detailed fetal neurosonography (TVS) and/or MRI are indicated in a case of cardiac rhabdomyoma. In a case of cardiac rhabdomyoma, confirmation of tuberous sclerosis is by demonstration of the cerebral lesions or by invasive testing for TSC1 or TSC2 gene mutations.

The cerebral tubers are seen as faintly hyperechoic nodules in the subependymal or cortical or subcortical regions. On MRI, the lesions are hypointense on T2-weighted imaging and iso- to hyperintense on T1-weighted imaging. MRI may demonstrate lesions undetected by ultrasonography (Figs. 4.20 and 4.21a–c). Like rhabdomyomas, the cerebral lesions are mostly seen later in gestation (after 24 weeks). Presence of intracranial lesions is confirmatory of tuberous

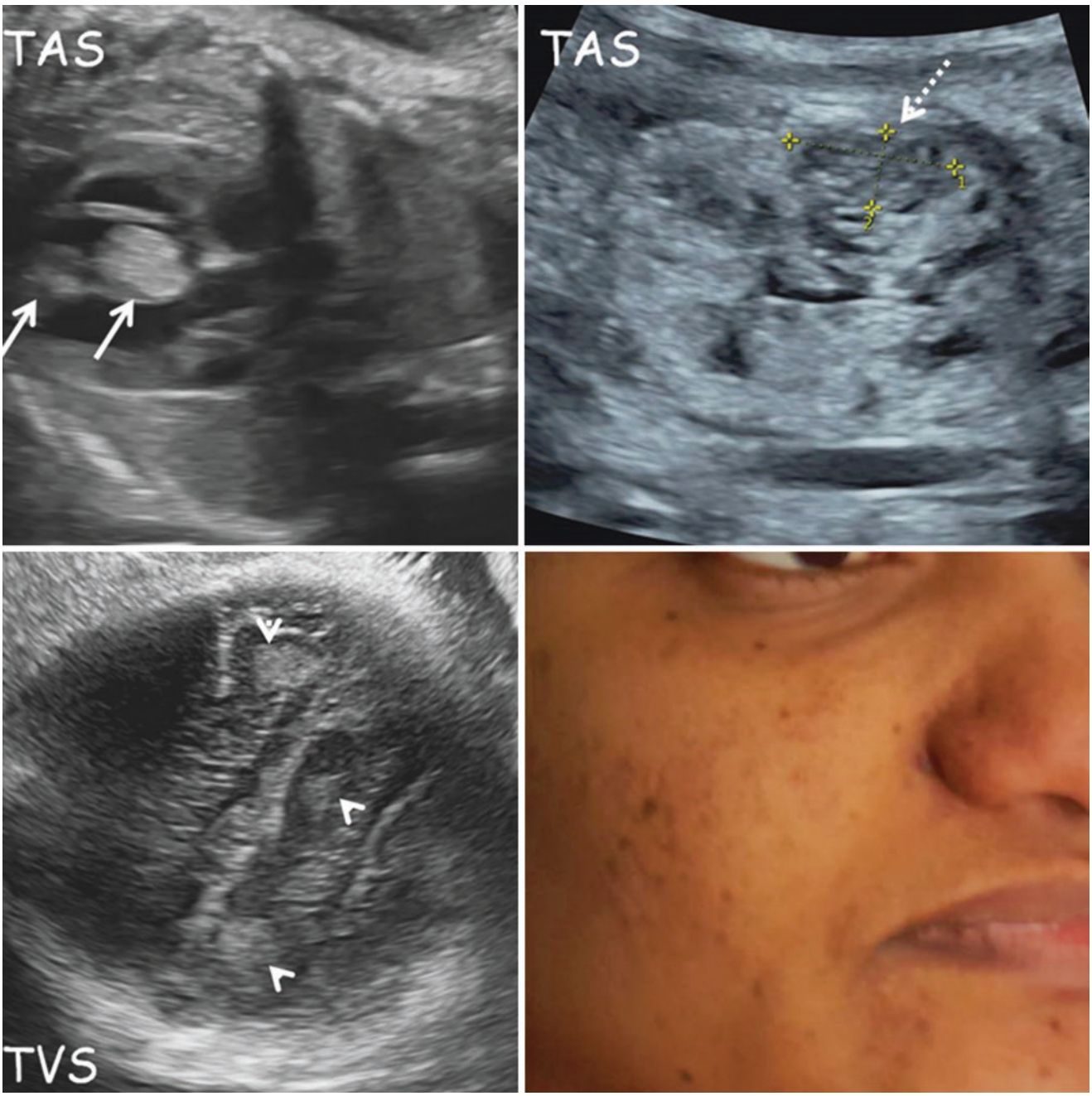

Fig. 4.20 32 weeks (TAS and TVS) *tuberous sclerosis* – four-chamber view, coronal section of the fetal right kidney, axial section superior to the transventricular plane, maternal face – multiple cardiac rhabdomyomas (solid arrows), fetal right renal convexity hypoechoic solid lesion possibly angiomyolipoma (dotted arrow), multiple bilateral cortical hyperechoic solid lesions, tubers (arrowheads), maternal facial adenoma sebaceum

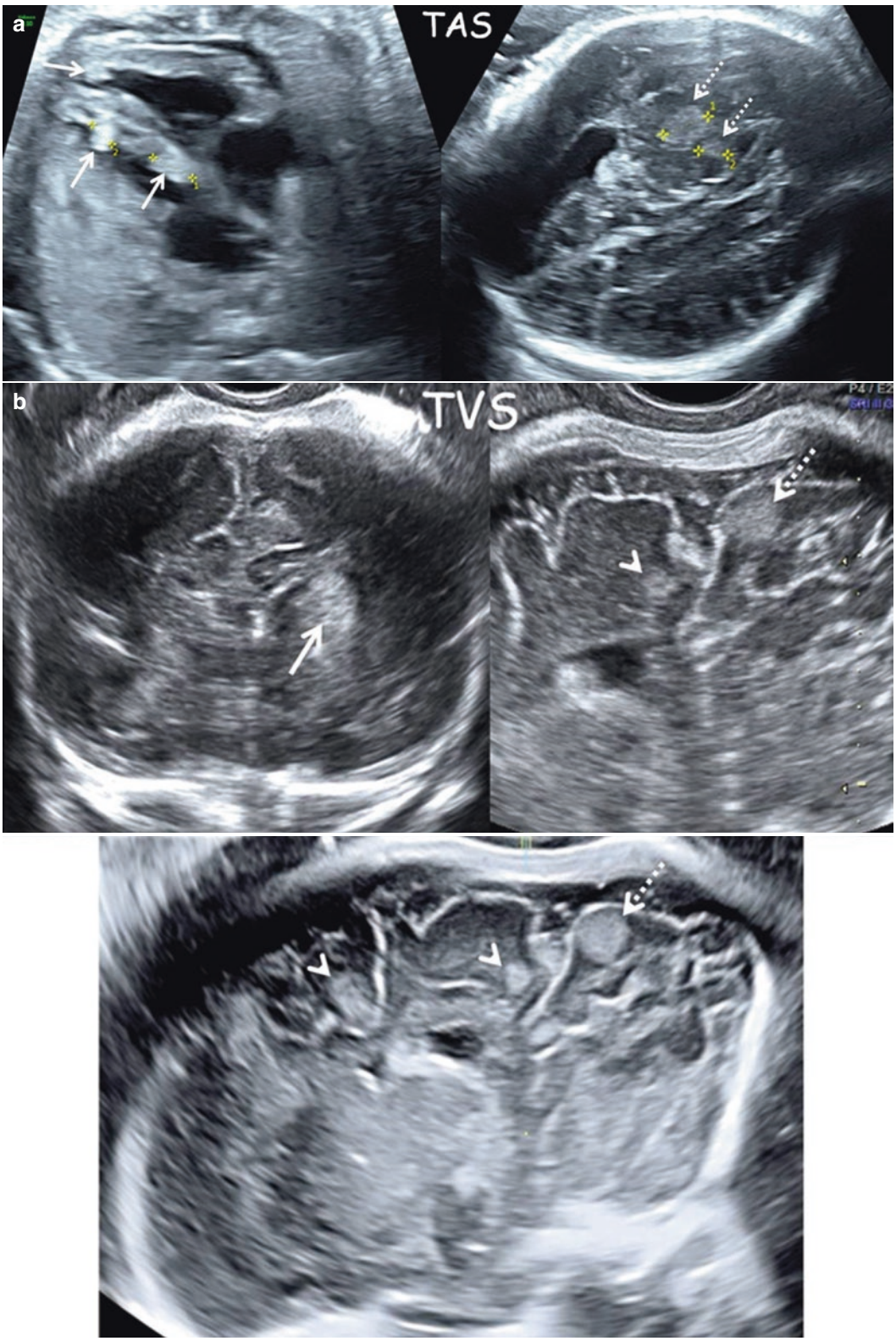

Fig. 4.21 (**a**) 32 weeks (TAS, TVS and MRI) *tuberous sclerosis* – four-chamber view and axial transventricular sections – multiple cardiac rhabdomyomas (solid arrows), faintly hyperechoic ovoid well-defined lesions, tubers in the left frontoparietal cortex (dotted arrows). (**b**) 32 weeks (TAS, TVS and MRI) *tuberous sclerosis* – coronal transcaudate, magnified left parasagittal and 3D multiplanar left parasagittal section with volume contrast imaging – left subependymal hyperechoic lesion, tuber (solid arrow), faintly hyperechoic ovoid well-defined lesions in the left frontal (arrowheads) and parietal cortex (dotted arrows). (**c**) 32 weeks (TAS, TVS and MRI) *tuberous sclerosis* – coronal transcaudate T2W and axial transventricular T1W images – left subependymal hypointense (solid arrow), faintly hyperintense ovoid well-defined lesion, tuber (dotted arrow)

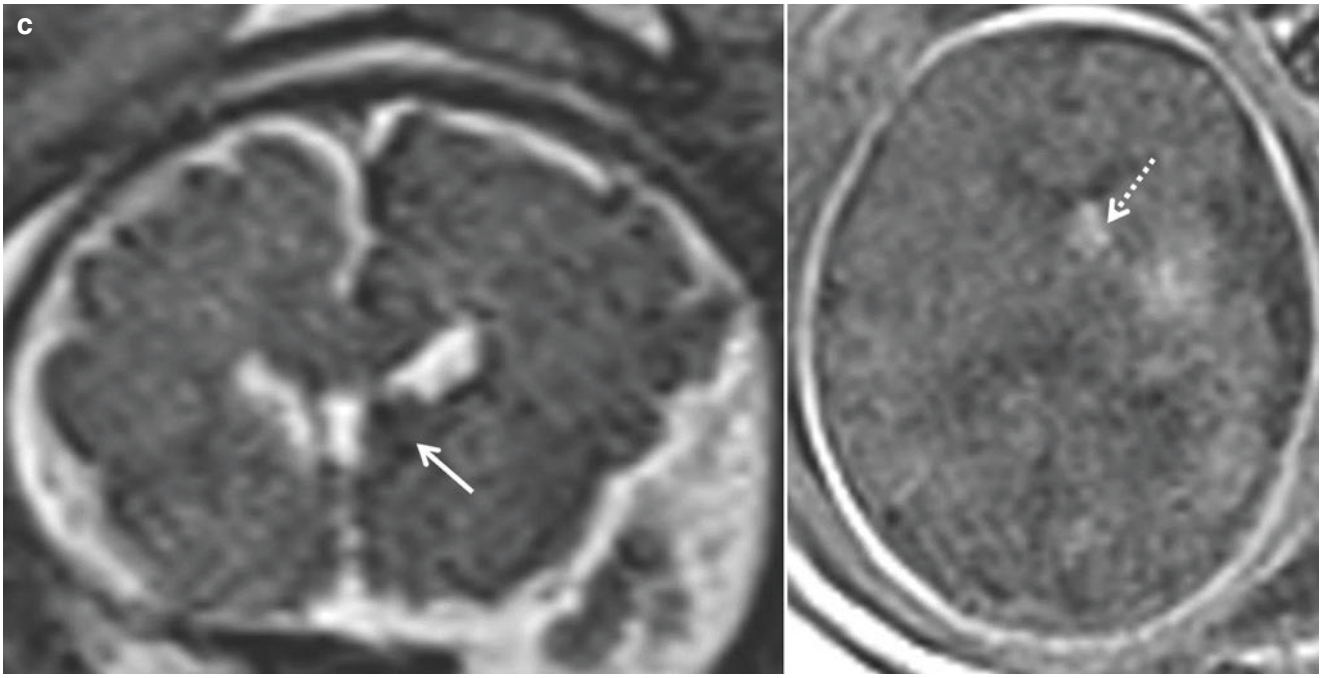

Fig. 4.21 (continued)

sclerosis. Absence of intracranial findings however does not rule out tuberous sclerosis.

Signs of tuberous sclerosis in the mother or father (facial cutaneous angiofibromas and renal angiomyolipomas) provide a clue to prenatal diagnosis. This can be supplemented by parental molecular testing.

4.3.2 Schizencephaly

Schizencephaly is characterised by a full thickness (transmantle) cerebral parenchymal cleft lined by grey matter. In type I (closed lip), the lips of the cleft are in contact with each other. In type II (open lip), the lips of the cleft are separated by a space filled with CSF. This results in a direct communication between the cerebral convexity subarachnoid space and the lateral ventricular lumen. Schizencephaly may occur as an isolated finding or in association with other intracranial anomalies (polymicrogyria, heterotopia, septal agenesis, focal cortical dysplasia or sulcation disorders) (Fig. 4.23a–g). It may be unilateral or bilateral.

The CSF-filled cerebral cleft is easily recognised if the separation of the lips is considerable. Closed-lip lesions generally escape prenatal detection. The lateral fissure is the most common site of the cleft (Figs. 4.22 and 4.23b, e–g). Fetal MRI helps diagnose the lesion in cases suspected on ultrasonography.

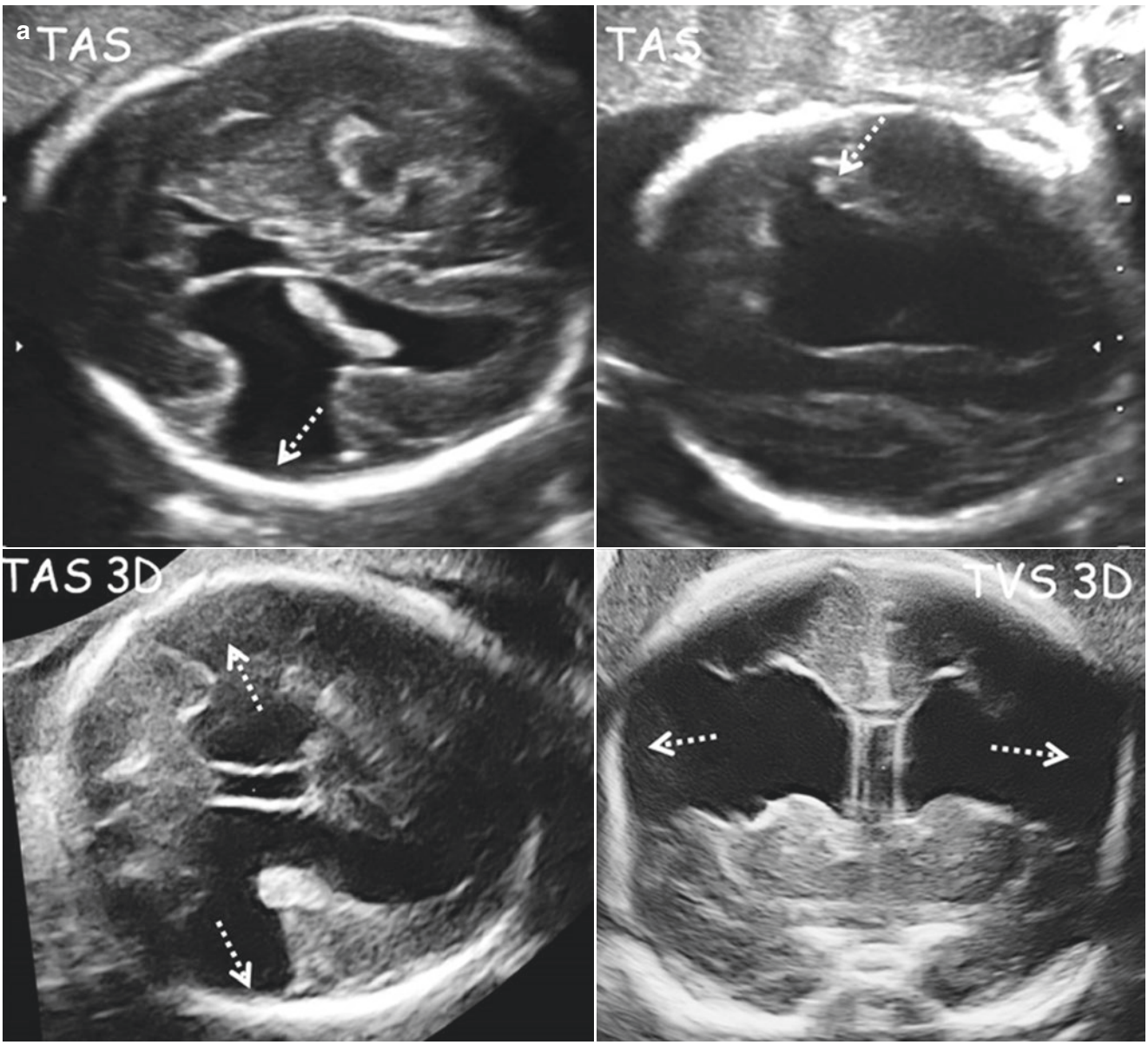

Fig. 4.22 (**a**) 28 weeks (TAS, TVS, 3D US) *bilateral open-lip schizencephaly with atretic cephalocele* – axial transventricular sections, 3D multiplanar axial transventricular section and coronal transcaudate sections – bilateral transmantle clefts (dotted arrows). The cleft in the near hemisphere is not well seen due to reverberation artefact in the direct transabdominal imaging. It is seen slightly better in section obtained from transabdominal and transvaginal 3D volumes. Also, note the bilateral lateral ventriculomegaly. (**b**) 28 weeks (TVS) *bilateral open-lip schizencephaly with atretic cephalocele* – midsagittal sections B mode and color Doppler – atretic cephalocele seen as a midline parietal region 3 × 4 mm scalp cyst with a narrow CSF tract connecting with the intracranium through a focal calvarial defect (solid arrow), persistent vertical embryonic position of the straight sinus reaching just anterior to the tract of the atretic cephalocele (dotted arrow). The absence of venous vascularity in the lesion connecting to the superior sagittal sinus differentiates it from sinus pericranii

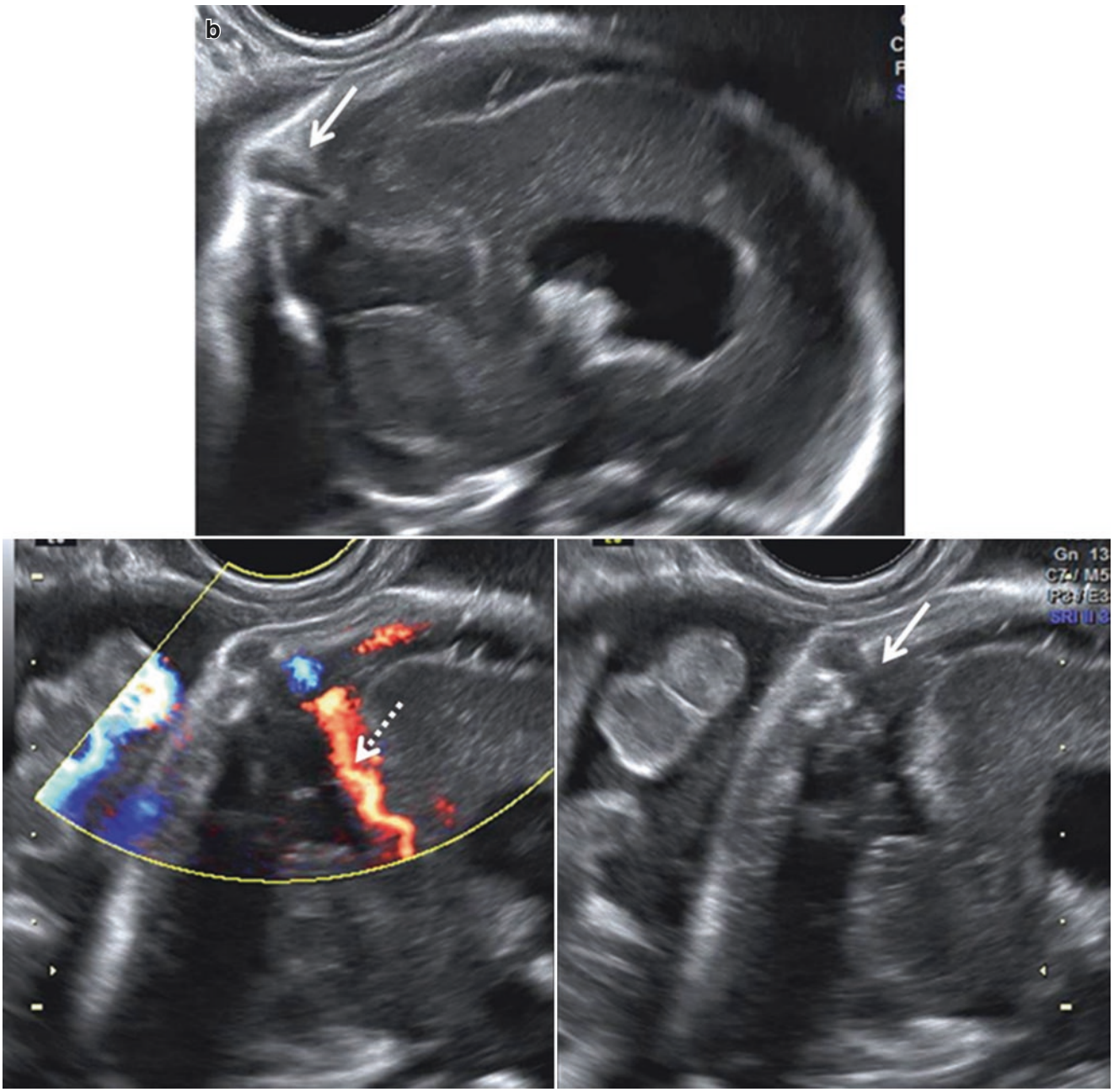

Fig. 4.22 (continued)

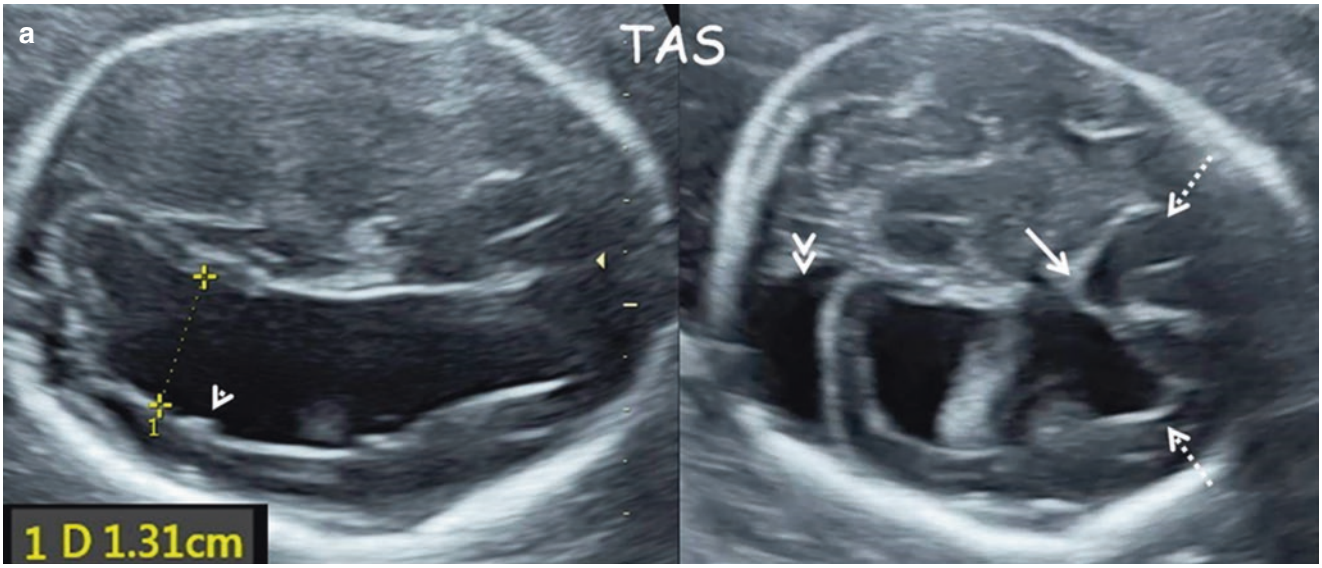

Fig. 4.23 (**a**) 21 weeks (TAS, TVS, 3D US and MRI) *right hemimegalencephaly, periventricular nodular heterotopia, open-lip schizencephaly, partial agenesis of CC, extra-axial fluid collection and sinus pericranii* – axial transventricular sections – right lateral ventriculomegaly (**), irregular lateral ventricular margins (arrowheads), CSP is not well seen (solid arrow), anterior horns are dysmorphic (dotted arrows), extra-axial right occipital fluid collection (double arrowheads). Note the right occipital lobe is transgressing the midline. This is due to larger volume of right cerebral hemisphere. (**b**) 21 weeks (TAS, TVS, 3D US and MRI) *right hemimegalencephaly, periventricular nodular heterotopia, open-lip schizencephaly, partial agenesis of CC, extra-axial fluid collection and sinus pericranii* – coronal transcaudate, right parasagittal sections (without and with magnification) – right cerebral hemisphere is larger, bilateral dilated dysmorphic anterior horns (*), thin body of CC (arrowhead), relatively thinner occipital cortex compared to frontal and parietal (double arrowheads), focal widening of adjacent subarachnoid space (**), transmantle occipital cortical defect (dotted arrow), irregular superior margin of right lateral ventricle (long-dotted arrow), subependymal nodules and contour abnormality of anteroinferior margin of right inferior horn (solid arrow), cystic scalp lesion overlying posterior fontanelle (dotted circle). (**c**) 21 weeks (TAS, TVS, 3D US and MRI) *right hemimegalencephaly, periventricular nodular heterotopia, open-lip schizencephaly, partial agenesis of CC, extra-axial fluid collection and sinus pericranii* – midsagittal and 3D midsagittal section with volume contrast imaging – body of the CC is seen (solid arrow), the rostrum, genu and splenium are not present, vermis (V). Note the right lateral ventricle is seen in the midsagittal plane. This is due to larger right hemisphere. (**d**) 21 weeks (TAS, TVS, 3D US and MRI) *right hemimegalencephaly, periventricular nodular heterotopia, open-lip schizencephaly, partial agenesis of CC, extra-axial fluid collection and sinus pericranii* – midsagittal section, 3D power Doppler rendered midsagittal image and comparable T2W section – midline scalp cystic lesion with vascular connection to the superior sagittal sinus, sinus pericranii. (**e**) 21 weeks (TAS, TVS, 3D US and MRI) *right hemimegalencephaly, periventricular nodular heterotopia, open-lip schizencephaly, partial agenesis of CC, extra-axial fluid collection and sinus pericranii* – 3D sectional multiplanar display – the navigation dot is in the transmantle cleft (open-lip schizencephaly). (**f**) 21 weeks (TAS, TVS, 3D US and MRI) *right hemimegalencephaly, periventricular nodular heterotopia, open-lip schizencephaly, partial agenesis of CC, extra-axial fluid collection and sinus pericranii* – right posterior horn rendered front back showing the schizencephaly cleft as a dark hole (solid arrow), irregular bumpy ependymal surface of right lateral ventricle (dotted arrow) (virtual ventriculoscopy). (**g**) 21 weeks (TAS, TVS, 3D US and MRI) *right hemimegalencephaly, periventricular nodular heterotopia, open-lip schizencephaly, partial agenesis of CC, extra-axial fluid collection and sinus pericranii* – comparison between the TVS and T2W axial transventricular and right parasagittal sections

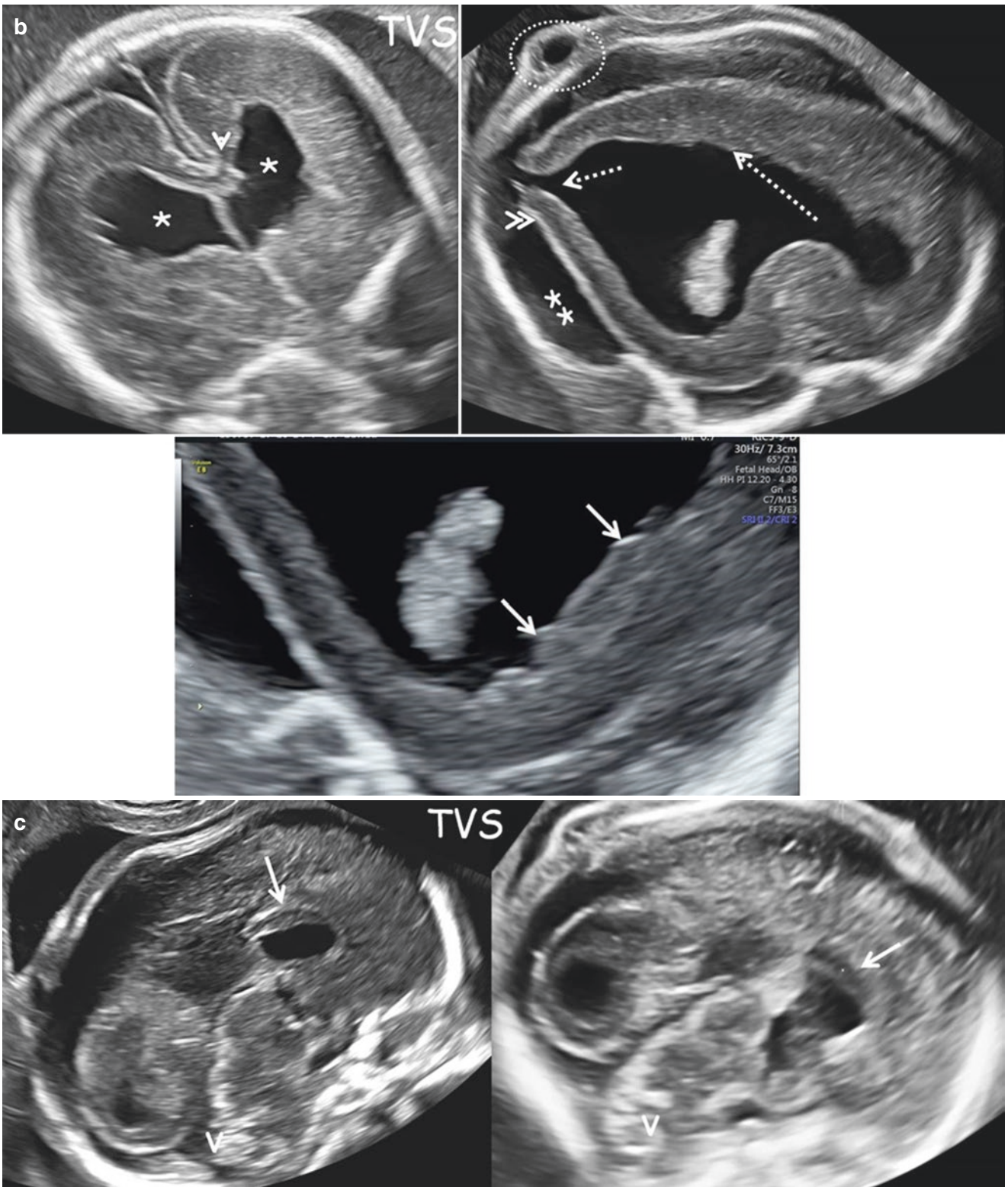

Fig. 4.23 (continued)

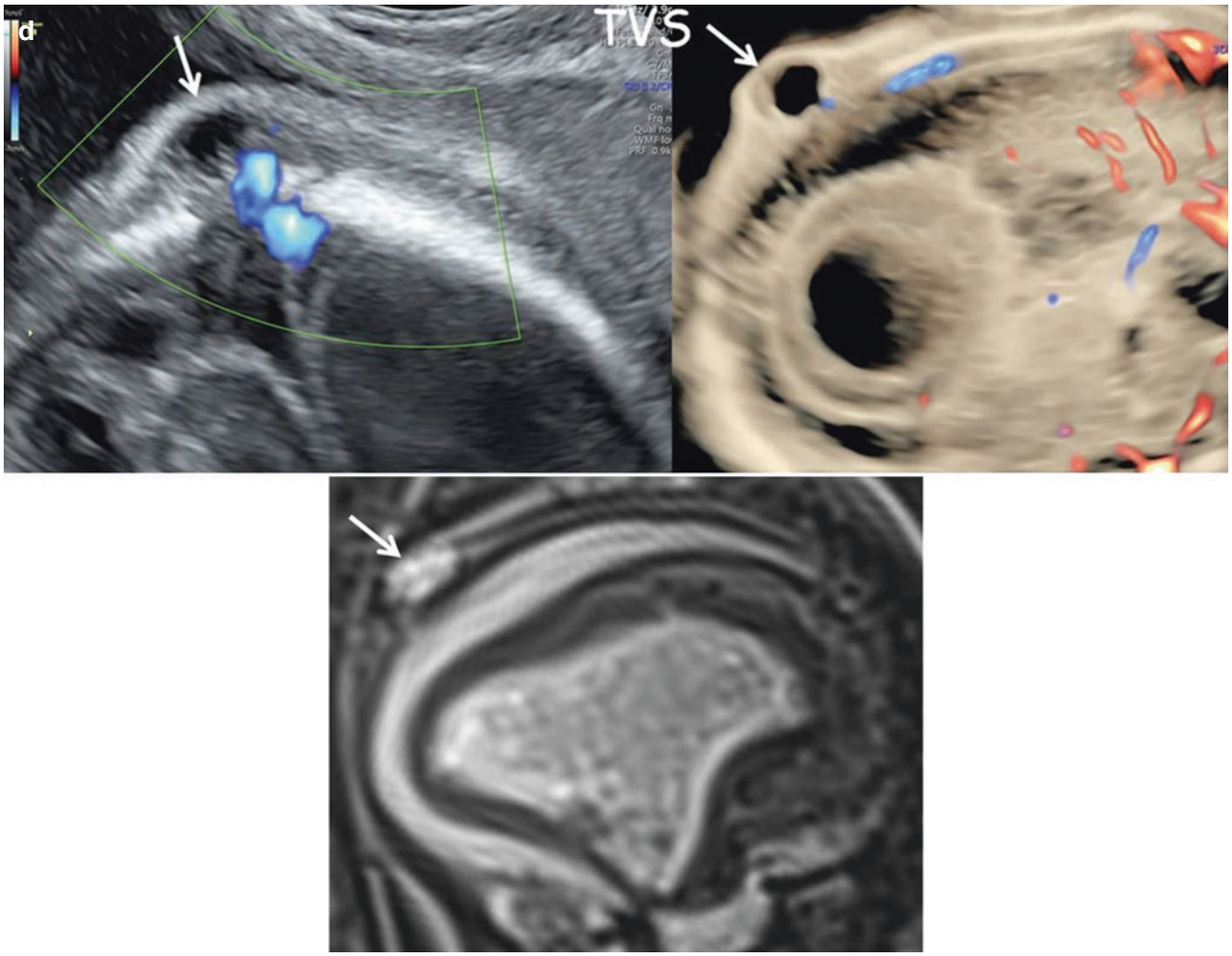

Fig. 4.23 (continued)

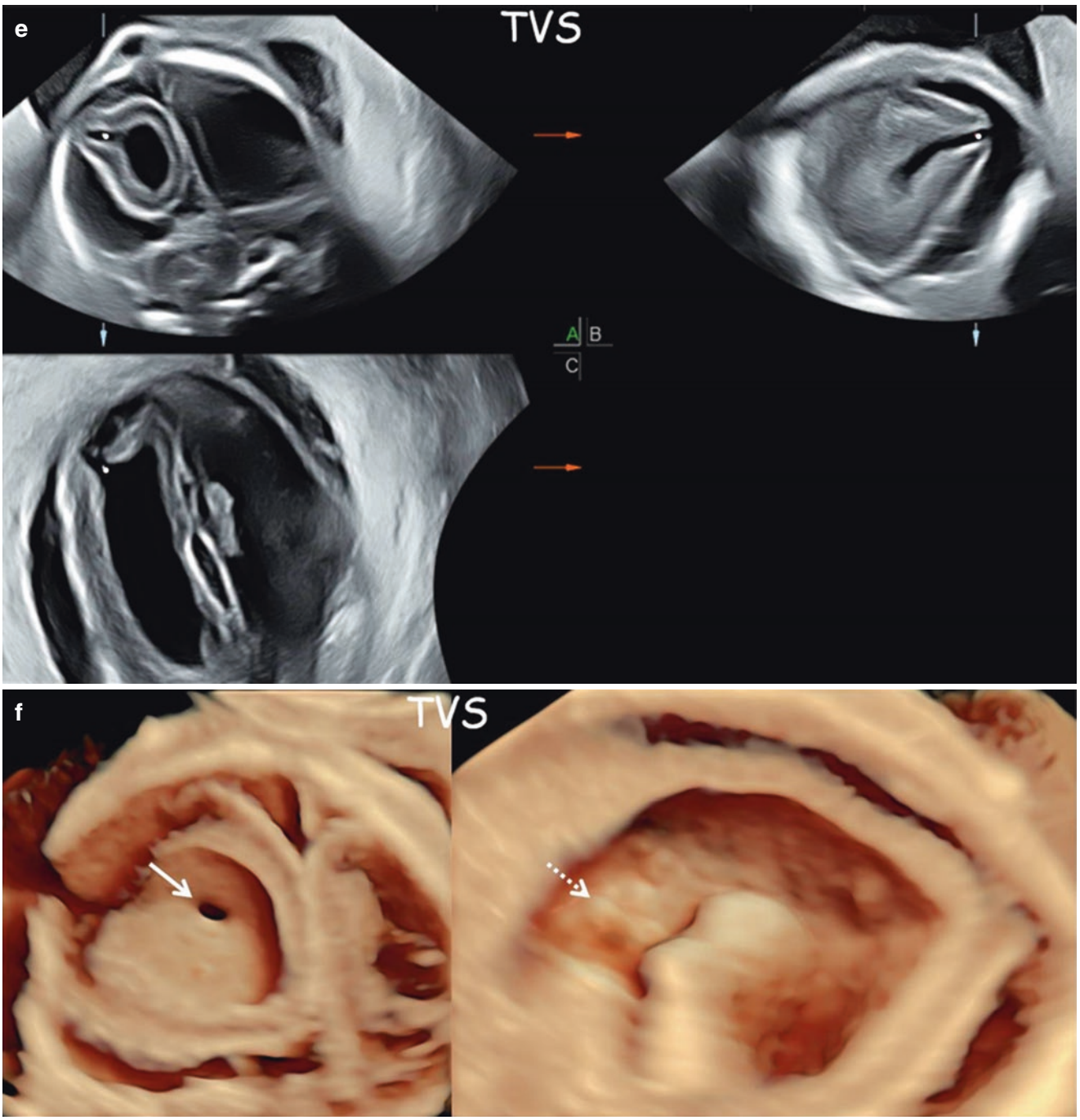

Fig. 4.23 (continued)

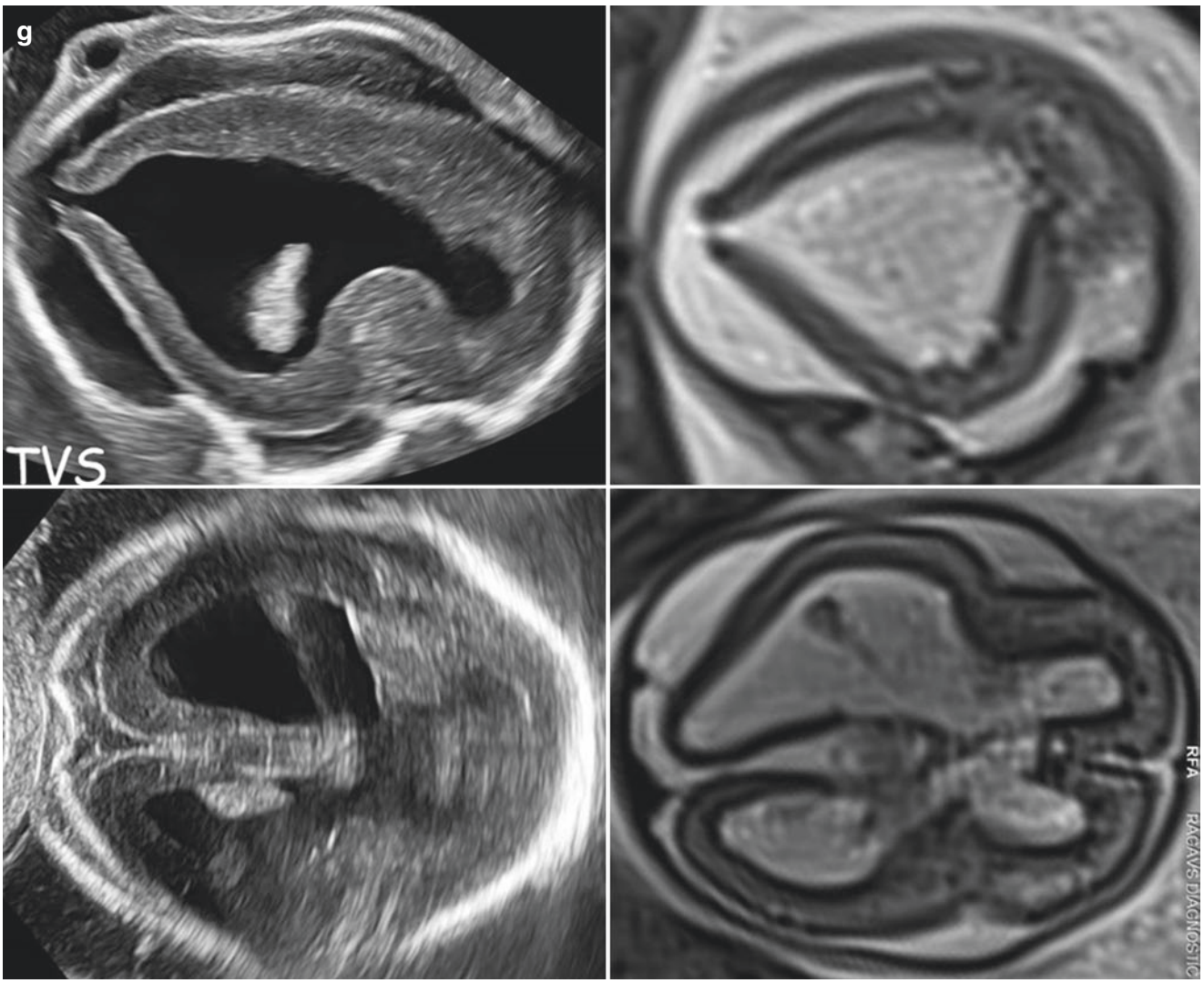

Fig. 4.23 (continued)

4.3.3 Polymicrogyria

Presence of tightly packed small gyri is the hallmark of polymicrogyria. Polymicrogyria (PMG) is caused by a genetic, infective or ischemic insult during the periods of neuronal proliferation, migration or organisation. In the fetus, it manifests as premature (prior to 26 weeks) cerebral convexity sulcation seen as surface undulations (Figs. 4.24 and 4.25). The typical cortical crinkling may be seen by ultrasonography in later gestation especially if there is increased cerebral convexity subarachnoid space as seen in fetal infection. PMG may affect only a part of the brain (unilateral focal PMG). The lesion is widespread in bilateral generalised PMG. It may be associated with septal agenesis, periventricular nodular heterotopia or schizencephaly. Fetal MRI is useful to confirm the cerebral convexity findings and also to detect associated abnormalities such as closed-lip schizencephaly and heterotopia.

To summarise, the whistle blower or the first finding in malformations of cortical development could be mild lateral ventriculomegaly, abnormal CSP, thin cortex, or micro- or macrocephaly. Any one of these signs is an indication for a detailed fetal neurosonogram preferably by transvaginal approach to diligently look for delayed/premature sulcation, ventricular bumpy margin/periventricular nodules, cortical nodules, corpus callosum abnormalities, thin cortex, increased subarachnoid space, cortical clefting, orbital abnormalities and other extracranial abnormalities. Fetal MRI confirms and supplements the ultrasound findings.

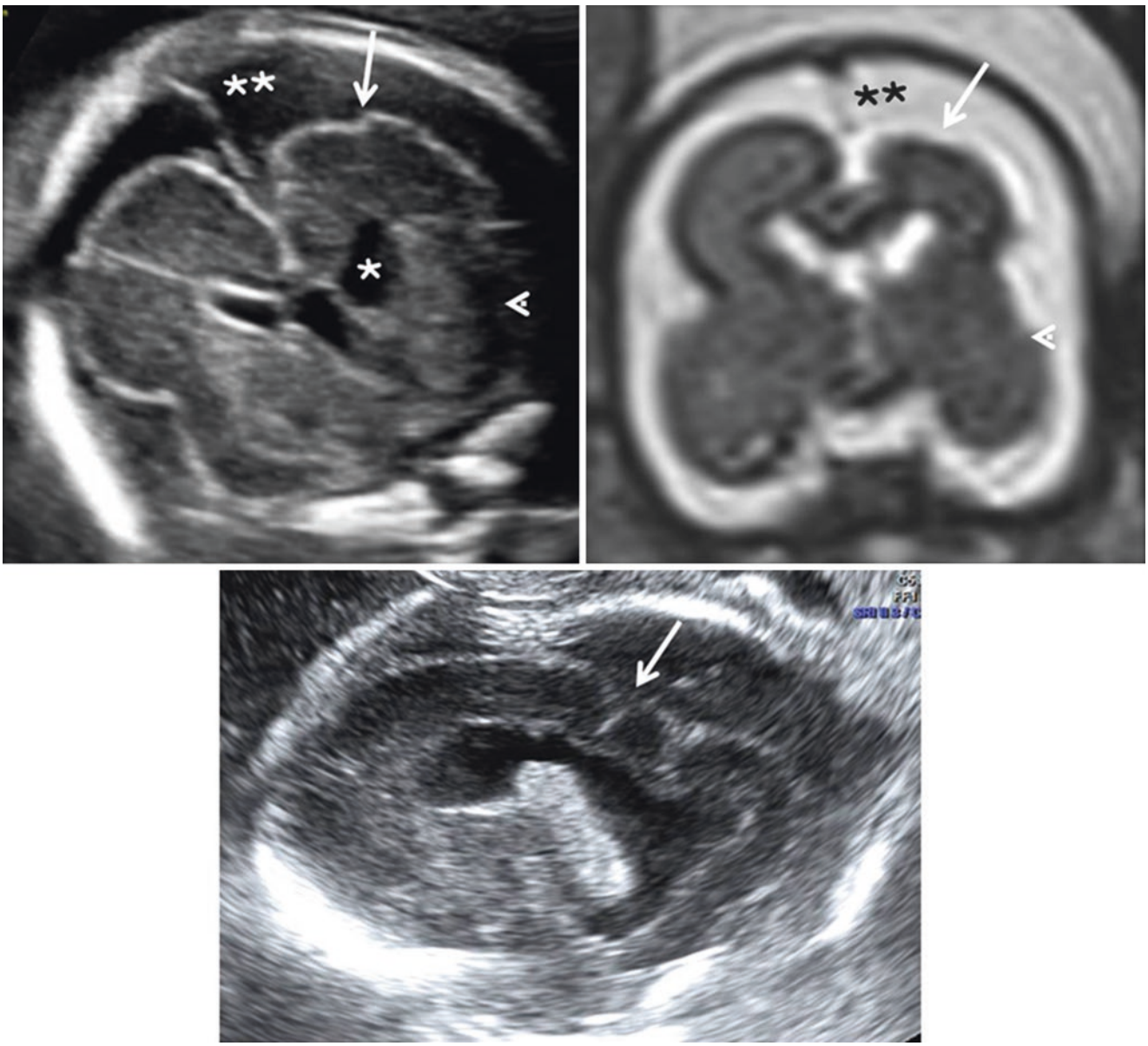

Fig. 4.24 23 weeks (TAS, TVS and MRI) *left polymicrogyria* – coronal transcaudate, left parasagittal sections and T2W MRI coronal transcaudate section – mild left lateral ventriculomegaly (*), left cerebral hemisphere is smaller (arrowhead) with increased subarachnoid space (**), polymicrogyria, premature appearance of convexity sulci (solid arrow)

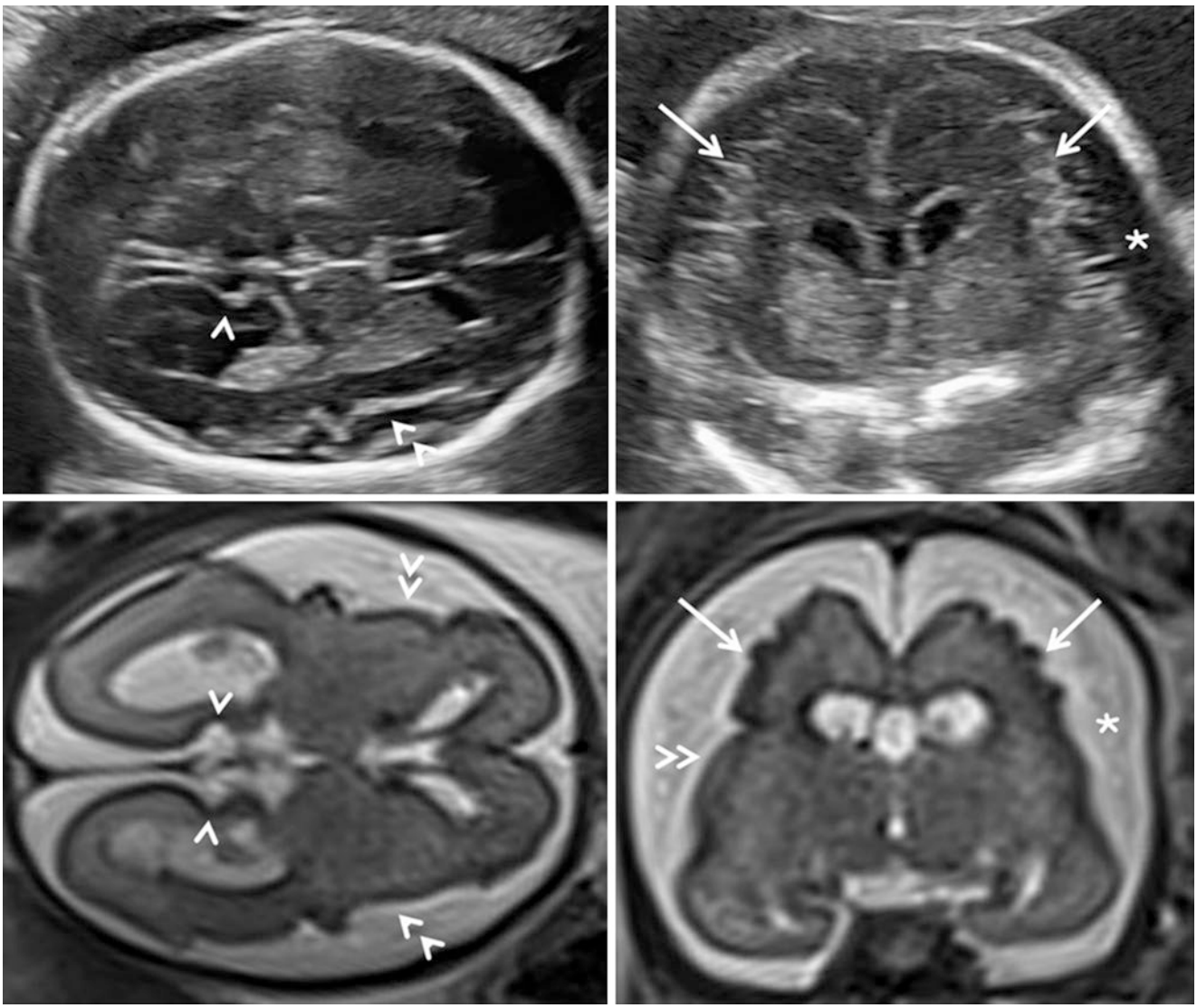

Fig. 4.25 26 weeks (TAS and MRI) *lissencephaly with polymicrogyria* – axial transventricular and coronal transcaudate US and T2W sections – delayed development of the parieto-occipital sulci (wider than deeper) (arrowheads), shallow, obtuse-angled lateral fissures (double arrowheads), crinkled appearance of cerebral convexity due to numerous small sulci and gyri (solid arrows) and prominent subarachnoid space (*)

Suggested Reading

1. Chervenak FA, Jeanty P, Cantraine F, Chitkara U, Venus I, Berkowitz RL, Hobbins JC. The diagnosis of fetal microcephaly. Am J Obstet Gynecol. 1984;149:512–7.
2. Leibovitz Z, Daniel-Spiegel E, Malinger G, Haratz K, Tamarkin M, Gindes L, Schreiber L, Ben-Sira L, Lev D, Shapiro I, Bakry H, Weizman B, Zreik A, Egenburg S, Arad A, Tepper R, Kidron D, Lerman-Sagie T. Prediction of microcephaly at birth using three reference ranges for fetal head circumference: can we improve prenatal diagnosis? Ultrasound Obstet Gynecol. 2016;47:586–92.
3. Chen CP, Chien SC. Prenatal sonographic features of Miller-Dieker syndrome. J Med Ultrasound. 2010;18:147–52.
4. Nagaraj UD, Hopkin R, Schapiro M, Kline-Fath B. Prenatal and postnatal evaluation of polymicrogyria with band heterotopia. Radiol Case Rep. 2017;12:602–5.
5. Dhombres F, Nahama-Allouche C, Gelot A, Jouannic JM, de Villemeur TB, Saint-Frison MH, le Pointe HD, Garel C. Prenatal ultrasonographic diagnosis of polymicrogyria. Ultrasound Obstet Gynecol. 2008;32:951–4.
6. Blondiaux E, Sileo C, Nahama-Allouche C, Moutard ML, Gelot A, Jouannic JM, Ducou le Pointe H, Garel C. Periventricular nodular heterotopia on prenatal ultrasound and magnetic resonance imaging. Ultrasound Obstet Gynecol. 2013;42:149–55.
7. Lacalm A, Nadaud B, Massoud M, Putoux A, Gaucherand P, Guibaud L. Prenatal diagnosis of cobblestone lissencephaly associated with Walker-Warburg syndrome based on a specific sonographic pattern. Ultrasound Obstet Gynecol. 2016;47:117–22.
8. Fong KW, Ghai S, Toi A, Blaser S, Winsor EJ, Chitayat D. Prenatal ultrasound findings of lissencephaly associated with Miller-Dieker syndrome and comparison with pre- and postnatal magnetic resonance imaging. Ultrasound Obstet Gynecol. 2004;24:716–23.